AD-A086 188 NATIONAL AERONAUTICS AND SPACE ADMINISTRATION MOFFET--ETC F/G 20/4
LARGE-SCALE WIND-TUNNEL TESTS OF INVERTING FLAPS ON A STOL UTIL--ETC(U)
JUN 80 T W FEISTEL, J P MORELLI

UNCLASSIFIED NASA-A-7061 NASA-TP-1696 NL

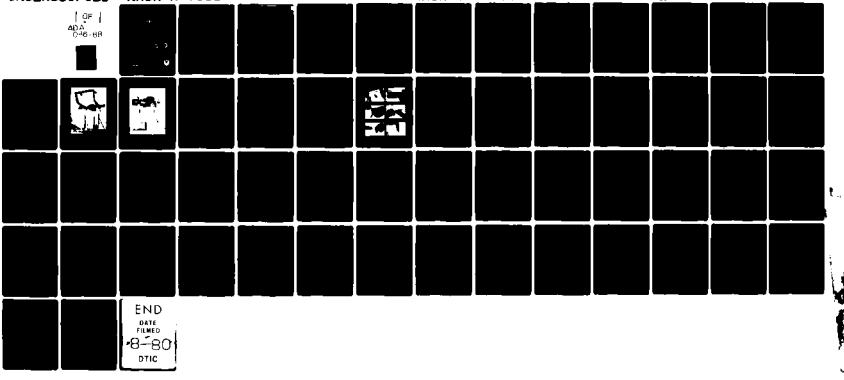

END
DATE FILMED
8-80
DTIC

NASA
Technical Paper 1696

AVRADCOM
Technical Memorandum 80-A-1

LEVEL II

Large-Scale Wind-Tunnel Tests of Inverting Flaps on a STOL Utility Aircraft Model

Terrell W. Feistel and Joseph P. Morelli

JUNE 1980

NASA

NASA
Technical Paper 1696

AVRADCOM
Technical Memorandum 80-A-1

Large-Scale Wind-Tunnel Tests of Inverting Flaps on a STOL Utility Aircraft Model

Terrell W. Feistel
Ames Research Center
Moffett Field, California

Joseph P. Morelli
Aeromechanics Laboratory
AVRADCOM Research and Technology Laboratories
Ames Research Center
Moffett Field, California

National Aeronautics
and Space Administration

**Scientific and Technical
Information Office**

1980

NOTATION

b	wing span
$\bar{c}$	mean aerodynamic chord
c	wing chord
C_D	drag coefficient, $\frac{D}{qS}$
c_F	flap chord
C_{H_F}	flap hinge-moment coefficient about flap pivot, $\frac{HM_F}{qS_F c_F}$
C_L	lift coefficient, $\frac{L}{qS}$
C_m	pitching-moment coefficient at 0.25 c, $\frac{M}{qSc}$
D	drag
HM_F	flap hinge-moment about flap pivot
i_H	horizontal tail incidence relative to wing chord plane, deg
L	lift
M	pitching moment
q	free-stream dynamic pressure
S	wing area
S_F	flap area per panel
T	thrust
T_c'	thrust coefficient, $\frac{T}{qS}$
α	angle of attack of wing chord plane, deg
γ	flightpath angle, deg
$\delta_{F/V}$	flap deflection, deg/vane deflection, deg
I/B	inboard
O/B	outboard

LARGE-SCALE WIND-TUNNEL TESTS OF INVERTING FLAPS ON A STOL UTILITY AIRCRAFT MODEL

Terrell W. Feistel
Ames Research Center

and

Joseph P. Morelli
Aeromechanics Laboratory
AVRADCOM Research and Technology Laboratories

SUMMARY

A unique inverting flap system has been investigated on a large-scale deflected slipstream model in the Ames 40- by 80-Foot Wind Tunnel. The term "inverting" is used because the flaps pivot about a point near the wing trailing edge and are retracted into the wing contour at a deflection approaching 180°. The subject tests utilized 33% chord double-slotted flaps on a low-aspect ratio wing that was fully immersed in the propeller slipstream. Evaluation of the flap effectiveness is aided by comparisons with the results of tests of other flap systems on the same twin propeller, twin tail boom STOL utility aircraft model.

No extreme or abrupt force or moment increments were encountered when the flaps were deflected through a wide range, corresponding to the complete retraction/extension spectrum. Hinge-moment information for the more important flap deflections was obtained from instrumented flap supports and exhibited acceptable behavior. Integral spoilers were investigated for lateral control and were found to produce appreciable rolling moments.

The lift and descent capability of the inverting flaps compared very favorably with that of other flap systems that have been tested on this model, including some with much greater mechanical complexity. As expected, the flaps caused large nose-down pitching moment increments at the high lift setting; however, the trimmed characteristics are still competitive with those obtained with the more complicated flap systems.

INTRODUCTION

The inverting flap concept was originated by Alberto Alvarez-Calderon (ref. 1), who designed the flaps used in the tests reported herein. "Inverting" flaps are large, chord extending flaps that pivot about a point near the wing trailing edge and are retracted into the wing contour at a deflection approaching 180°. One of the principal differences (as elaborated in ref. 1) between inverting flaps and the more common types of chord-extending flaps is in their potentially simpler (and lighter) method of mounting and installation, presumably requiring only a pivot and an extensible

cable. Other significant differences include the potential rapid retract and deployment capabilities and the wide range (0° to 180°) of settings possible.

The subject wind-tunnel tests were initiated to shed light on some of the unanswered questions regarding the practical use of these flaps. In particular, the potential problems associated with trimming such large chord-extending flaps, possible undesirable aerodynamic force and moment transients during deployment and retraction of the flaps, and the magnitude of the hinge moments encountered, were investigated.

DESCRIPTION OF THE MODEL

The model with flaps deflected is shown mounted in the wind tunnel in figure 1. It represents, in approximately full scale, a generalized twin propeller, twin tail boom, deflected slipstream STOL utility aircraft. A three-view sketch of the model is shown in figure 2(a). Figures 2(b) and 2(c) show typical airfoil and flap cross sections, and spoiler and end plate details, respectively. The flap and airfoil coordinates are given in table 1. Close-up photographs of the flap segments set at various deflections are shown in figure 3. Further details of the model may be found in reference 2.

TESTS

Tests to determine the longitudinal characteristics of the model were made for flap/vane deflections ($\delta_{F/V}$) of 20/9.5, 40/21, 60/32, 120/13.5, 180/0, and 60/32 inboard – 90/37 outboard, with a nominal free-stream dynamic pressure of 192 N/m^2 (4 psf) and with nominal thrust coefficients of 0, 1, 2.4, and 4 at most of the deflections. The data are referenced to wind axes for the forces and to stability axes for the moments. Except as noted in the "Discussion and Analysis" section, the data are computed about the 25% wing mean aerodynamic chord position on the wing chord line. The nominal Reynolds number based on the wing mean aerodynamic chord of 2.13 m (7.0 ft) was 2.53×10^6.

The data are not corrected for model support strut tares or for wind-tunnel wall effects. For this support strut system, experience has shown that the tares are negligible for high lift configurations. As a basis of comparison for tunnel wall effects, a representative calculation was made using the $C_{L_{aero}}$ method (cf. ref. 3, p. 9), in which the classical corrections are applied to the circulation portion of the lift only (after subtracting an estimate of the reaction lift attributable directly to thrust). Approximate corrections for the assumed representative maximum performance descent condition ($C_L = 6$ at $\gamma = -10°$, $T_c' = 2$) are as follows:

$$\left.\begin{aligned} \Delta\alpha &= +1.7 \\ \Delta C_D &= +0.12 \\ \Delta C_M &= +0.07 \text{ (tail on)} \end{aligned}\right\} \qquad (1)$$

TABLE 1.– INVERTING FLAP SYSTEM

(a) Main wing airfoil ordinates in fraction of wing chord. (Model scale wing chord length c = 2.13 m (84 in.); basic airfoil section NACA 63A–418 (a = 0.8 mod); leading-edge radius 0.0235 c on slope through leading edge of 0.1860.)

Upper surface		Lower surface	
x/c	y/c	x/c	y/c
0.0023	0.0153	0.0077	0.0131
.0045	.0187	.0105	-.0155
.0090	.0243	.0160	-.0195
.0209	.0349	.0291	-.0265
.0453	.0504	.0547	-.0360
.0701	.0621	.0799	-.0426
.0951	.0717	.1049	-.0478
.1453	.0868	.1547	-.0555
.1957	.0979	.2043	-.0607
.2463	.1060	.2537	-.0640
.2970	.1115	.3030	-.0656
.3477	.1144	.3523	-.0654
.3984	.1148	.4016	-.0636
.4491	.1129	.4509	-.0603
.4998	.1089	.5002	-.0557
.5504	.1032	.54	-.0503
.6010	.0959	.55	-.0484
.6515	.0872	.56	-.0460
.7019	.0772	.58	-.0390
.7522	.0664	.60	-.0301
.8026	.0546	.65	-.0105
.8525	.0415	.69	.0051
.87	.0375	.71	.0128
.88	.0345	.73	.0197
.89	.0315	.75	.0249
.90	.0282	.80	.0319
.91	.0249	.85	.0343
		.86	.0341
		.87	.0334
		.88	.0319
		.89	.0297
		.90	.0270
		.91	.0240

Pivot points:	x/c	y/c
Flap:	0.9468	0.0024
Vane:	.8770	-.0101

TABLE 1.– CONTINUED.

(b) Flap ordinates in fraction of flap chord. (Model scale flap chord length 0.71 m, 0.33 c (28 in.); leading-edge radius 0.035 c_{flap} on chord line.)

x/c_{flap}	y_{upper}/c_{flap}	y_{lower}/c_{flap}
0	0	0
.0135	.0290	-.0260
.025	.0410	-.0345
.050	.0550	-.0430
.075	.0640	-.0495
.10	.0701	-.0535
.15	.0760	-.0600
.20	.0765	-.0660
.25	.0745	-.0715
.30	.0690	-.0755
.35	.0645	-.0780
.40	.0590	-.0770
.45	.0540	-.0735
.50	.0490	-.0680
.60	.0390	-.0548
.70	.0290	-.0395
.80	.0190	-.0235
.90	.0090	-.0095
.95	.0045	-.0040
1.0	0	0

Flap pivot point:	x/c_{flap}	y/c_{flap}
	-0.210	0.098

TABLE 1.– CONCLUDED.

(c) Vane ordinates in fraction of vane chord. (Model scale vane chord length 0.25 m, 0.12 c (10 in.); leading-edge radius 0.038 c_{vane} on chord line.)

x/c_{vane}	y_{upper}/c_{vane}	y_{lower}/c_{vane}
0	0	0
0.0125	0.0580	-.0360
.0250	.0790	-.0490
.050	.1120	-.0580
.075	.1340	-.0600
.10	.1520	-.0580
.15	.1770	-.0510
.20	.1990	-.0480
.25	.1990	-.0420
.30	.2000	-.0355
.35	.1950	-.0300
.40	.1810	-.0240
.45	.1700	-.0190
.50	.1540	-.0130
.60	.1240	-.0020
.70	.0940	.0090
.80	.0640	.0185
.85	.0490	.0190
.90	.0340	.0140
.95	.0190	.0040
1.00	.0040	-.0040

Vane pivot point:	x/c_{vane}	y/c_{vane}
	0.0210	-0.0865

It is conceded that such corrections (for an extreme condition) are not negligible. But they are not of such a magnitude as to invalidate the conclusions drawn by examining the uncorrected data. The data are presented in uncorrected form in order to be directly comparable with the previously published data for the same and similar models (ref. 2). Wall corrections can be applied to the data using the classical method as follows:

$$\left.\begin{aligned} \alpha &= \alpha_u + 0.4355\, C_{L_u} \\ C_D &= C_{D_u} + 0.0076\, C_{L_u} \end{aligned}\right\} \tag{2}$$

and, with the tail on

$$C_M = C_{M_u} + 0.0175\, C_{L_u} \tag{3}$$

where the subscript u indicates data uncorrected for wall effects.

Propeller thrust was determined by taking the difference between longitudinal force measurements with propellers operating and with propellers removed. Propeller thrust measurements were made at several propeller speeds for each of three free-stream dynamic pressures with the flaps retracted and with the model at the angle of attack for zero lift. The propellers were contrarotating and propeller rotation was down inboard for all of the tests. Details concerning the propeller design may be found in reference 2.

To obtain flap hinge-moment data, the flap positioning links on the right wing were fitted with strain gauges. The integral spoiler was installed in the right outboard panel only, as shown in figures 2(a) and 2(c) and was deflected 40° from the nesting position for the lateral control effectiveness tests. The horizontal stabilizer was pivoted at the top of the vertical fins and was set at several discreet angles as noted. The integral hinged elevator was set at zero with respect to the stabilizer throughout the tests.

RESULTS

An index to the basic data figures is presented in table 2. The basic data are presented without discussion. Figures 4 through 8 present data for a range of flap settings, both tail off and tail on at various stabilizer settings. Figure 9 shows the effect of a spanwise variation in flap deflection (hybrid setting), and figure 10 presents results obtained with a partially folded flap position ($\delta_{F/V} = 120°/13.5$). The plane wing characteristics ($\delta_{F/V} = 180°/0$) are presented in figure 11.

The effects of spoiler deflection for roll control are shown in figure 12 for two flap settings ($\delta_{F/V} = 60/32$ and 90/37). The simple spoilers tested are capable of providing more than adequate rolling moments, that are relatively invariant with C_L for constant T_c'.

TABLE 2.– INDEX TO DATA FIGURES

Figure	$\delta_{F/V}$	$i_H{}^a$	T_c'	Remarks
4(a)	60/32	–	(0,1,2.4,4)	Tail off
4(b)	↓	+5	(0,1.1,2.3,3.9)	
4(c)	↓	-5	(0,1,2.4,4)	
4(d)	↓	-15	(0,1,2.4,4)	
5(a)	40/21	–	(0,1,2.4,4)	Tail off
5(b)	40/21	+5	(0,1.1)	
6(a)	20/9.5	–	(0,1,2.4,4)	Tail off
6(b)	20/9.5	+5	(0,1,2.4)	
6(c)	20/9.5	-10	(0,1,2.4,4)	
7(a)	90/37	–	(0,1,2.4,4)	Tail off
7(b)	90/37	+5	(0,1.1,2.4,4)	
7(c)	90/37	-10	(0,1,2.4,4)	
8	90/21	-10	(0,1,2.4,4)	
9	60/32 *I/B* 90/37 *O/B*	-10	(0,1,2.4,4)	Hybrid setting
10	120/13.5	+5	(0,1.1,2.4)	
11	180/0	+5	(0,1.1)	Stored position
12(a)	60/32	-15	(0,1,2.4,4)	40° spoiler, rt. wing O./B. (lat.-direc. data)
12(a) concl	60/32	-15	↓	40° spoiler, rt. wing O./B. (long. data)
12(b)	90/37	-10	↓	40° spoiler, rt. wing O./B. (lat.-direc. data)
12(b) concl	90/37	-10	(0,1,2.4,4)	40° spoiler, rt. wing O./B. (long. data)
13(a)	20/9.5	+5	(0,1,2.4)	Flap hinge movements (rt.)
13(b)	40/21	↓	(0,1.1)	↓
13(c)	60/32	↓	(0,1.1,2.3,3.9)	↓
13(d)	90/37	↓	(0,1.1,2.4,4)	↓
13(e)	120/13.5	↓	(0,1.1,2.4)	↓

[a]Elevator deflection zero with respect to stabilizer, all runs.

The flap hinge-moment data are presented in figure 13. The static hinge moments fall within a reasonable range for all flap deflections, indicating that no significant structural problems should be encountered, provided the deployment sequence is programmed to avoid high impact loads. No negative (compressive) loads were detected under any test condition, indicating that simple extensible cables should suffice to position the flaps.

DISCUSSION AND ANALYSIS

Potential Performance Capabilities

Figure 14 shows a representative set of polars for a hypothetical STOL airplane, similar to the wind-tunnel model, with inverting flaps set at 60/32. The wind-tunnel data have been adjusted for a trimming tail load with the c.g. set at 0.35 c on the thrust line.

Several sets of constant-value lines for a wing loading of 2394 N/m^2 (50 psf) are superimposed on the basic polars in this figure. Radiating from the origin are lines of constant descent angle, γ. The curved dashed line from the origin represents a sink rate of 6.10 m/s (20 fps), which is a nominal landing gear limit for this type of aircraft. For reference, horizontal lines of constant approach speed are shown. The hatched lines are approximate boundaries of constant "no-flare" landing distance[1] over a 15.2-m (50-ft) obstacle.

A shaded circle is superimposed to indicate a potentially feasible landing approach condition for a 152-m (500-ft) landing. This corresponds to an approach speed of 50 knots (C_L = 5.9) and a descent angle of approximately 10° (C_D = 1.03). The thrust coefficient would approximate 2.0 (approximately 800 total SHP (59,656 W)), and the angle of attack would approximate 15° (nose-up attitude of 5°) for the hypothetical STOL airplane. The approach rate of sink in this condition would be approximately 4.5 m/s (15 fps).

Comparison With Other Flap Systems

Figure 15 compares the relative descent performance for three different high lift systems: a simple double-slotted flap; a rotating cylinder flap; and the inverting flaps. All three fold into the same basic wing contour for cruise and have been tested in the Ames 40- by 80-Foot Wind Tunnel using this same STOL utility aircraft model with the same basic wing planform and propulsion system. The rotating cylinder flap system is the most mechanically complicated, being a form of mechanical boundary-layer control, and is described in reference 2.

As a basis for comparison (assuming a 2394 N/m^2 (50 psf) wing loading throughout), a representative maximum usable descent condition is shown for each flap system. The descent angle of

[1] The hypothetical "no-flare" landing distances are based on a straight approach path over a 15.2-m (50-ft) obstacle to touchdown, followed by a constant 0.5 g linear deceleration to stop. They are meant only as a guide to potential maximum performance STOL landing capability, which can be easily superimposed on the polar plot. The "no-flare" landing distances, as calculated, correspond very closely to flight-test data for actual "half-flare" landings in current generation STOL aircraft, as shown in reference 4; they serve, therefore, as a valid basis for comparison.

attack is arbitrarily chosen as 10° below the angle of attack for maximum lift. Shown superimposed are the constant, no-flare landing distance lines introduced in the previous figure. The rotating cylinder flap and the inverting flap are seen to be quite evenly matched at a descent angle of approximately 13° to 14°, corresponding to a theoretical "no-flare" landing distance of about 122 m (400 ft) over a 15.2-m (50-ft) obstacle. The double-slotted flap system (with much less chord extension) has about one-half this maximum descent capability, with a descent angle of 7° to 8°, corresponding to a distance of about 183 m (600 ft).

Summary of Longitudinal Data for a Range of Flap Settings

Figure 16(a) summarizes, for $T_c' = 1.0$, longitudinal data (at $i_H = +5°$) covering the complete range of flap settings tested. It can be seen that no extremely abrupt force or moment changes are encountered in going from the 180° folded position to one of the lifting positions (20° to 90°) and back again.[2] Figure 16(b) shows, for reference, a pitching moment plot of the same data recomputed with the moment reference located at 0.25 $\bar{c}$ longitudinally but, more appropriately, on the thrust line instead of on the wing chord. It will be noticed that some of the pitching moment curves have their positions shifted with respect to each other, but no large effects are involved.

Longitudinal Stability and Trim Considerations

In order to evaluate more easily the longitudinal stability and trim considerations involved in using such highly effective flaps, the data have been recomputed with respect to a c.g. on the thrust line at the 0.35 c point. This is a more representative location for a deflected slipstream STOL aircraft.

Figure 17(a) is a summary plot with the moment reference at 0.35 c on the thrust axis. It shows the pitching moment curves for the complete range of flap settings with $T_c' = 1$ and $i_H = +5°$. (Data were available for all flap settings at $i_H = +5°$. More nose-up trim is, of course, available at the more negative stabilizer settings.) It can be seen that, except for the $\delta_F = 120°$ transition position, all flap settings exhibit positive or neutral stability throughout the usable angle-of-attack range for these conditions.

To facilitate analyses with reference to this c.g. location, figures 17(b) through 17(e) show representative pitching-moment characteristics for flap deflections of 60/32 ($i_H = -5°$), 90/37 ($i_H = -10°$), 60/32 inboard – 90/37 outboard ($i_H = -10°$), and 20/9.5 ($i_H = -10°$), covering a wide range of thrust coefficients with the reference at 0.35 c on the thrust axis. Figure 17(f) shows representative tail-off pitching-moment data about this reference at $T_c' = 2.4$ for three flap settings: 60/32, 90/37, and 20/9.5.

It is obvious that the horizontal tail used on the wind-tunnel model was not adequate to trim these flaps at their most effective settings. In fact, it was far from optimum for a high-performance STOL aircraft; it was relatively small, poorly end plated, and had a simple nonslotted control surface (which was not deflected for this test).

[2] It is anticipated that the $\delta_F = 120°$ position would not be used for steady-state flight, but that the flap would be moved continuously through such transition positions to arrive at the more effective deflections.

A preliminary study indicated that the standard horizontal tail of the OV-10A aircraft would be adequate for trimming the pitching moments produced by the $\delta_F = 60/32$ inverting flap configuration reported herein up to a T_C' of 2.4, with a maneuvering reserve capability of about 0.6 rad/sec^2. A slightly larger horizontal tail would be required to provide adequate trim and maneuver capability up to $T_C' = 4$.

CONCLUDING REMARKS

Tests have been performed on a full-scale, twin-boom deflected slipstream STOL utility aircraft configuration equipped with "inverting" flaps in the Ames 40- by 80-Foot Wind Tunnel. The results show that the lift and descent capability provided by these flaps compares favorably with that of other flap systems that have been tested on the same model, including some with much greater mechanical complexity.

In spite of a large tail-off nose-down pitching moment produced by the inverting flaps in the highest lift configurations, the trimmed characteristics are competitive with those obtained from the more complicated flap systems. The flap hinge moments exhibited acceptable behavior throughout the range of deflections tested.

It is believed that these flaps may have promising potential application to the design of relatively simple STOL utility aircraft with improved performance capabilities. In addition, they may merit consideration as retrofits to existing aircraft with less effective flap systems.

Ames Research Center
National Aeronautics and Space Administration
Moffett Field, Calif. 94035, February 1980

REFERENCES

1. Alvarez-Calderon, Alberto: Design and Tests of Inverting Flaps and Wing Span Flaps. S.A.E. Paper No. 680646 presented at the Aeronautics and Space Engineering and Manufacturing Meeting, Los Angeles, Calif., Oct. 1968.

2. Weiberg, J. A.; and Gamse, Berl: Large-Scale Wind Tunnel Tests of an Airplane Model with Two Propellers and Rotating Cylinder Flaps. NASA TN D-4489, 1978.

3. Koenig, D. G.; and Corsiglia, V. R.: Aerodynamic Characteristics of a Large-Scale Model with an Unswept Wing and Augmented Jet Flap. NASA TN D-4610, 1968.

4. Feistel, T. W.; and Innis, R. C.: Results of a Brief Flight Investigation of a COIN-Type STOL Aircraft, NASA TN D-4141, 1967.

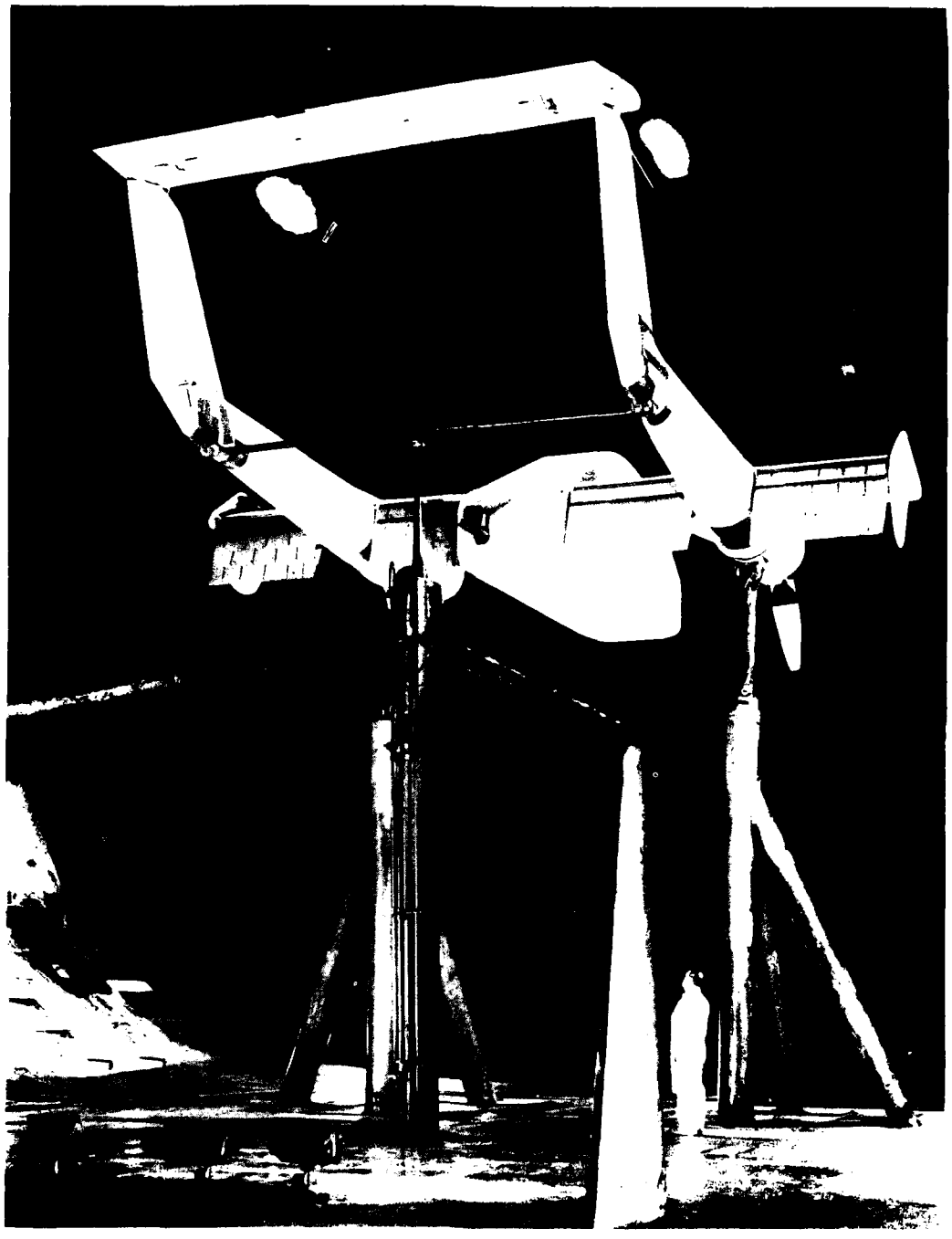

(a) Three-quarter rear view, $\delta_{F/F} = 60/32$.

Figure 1. Photos of model mounted in tunnel.

(b) Three-quarter front view, $\delta_{F,T} = 60°32'$.

Figure 1. Concluded.

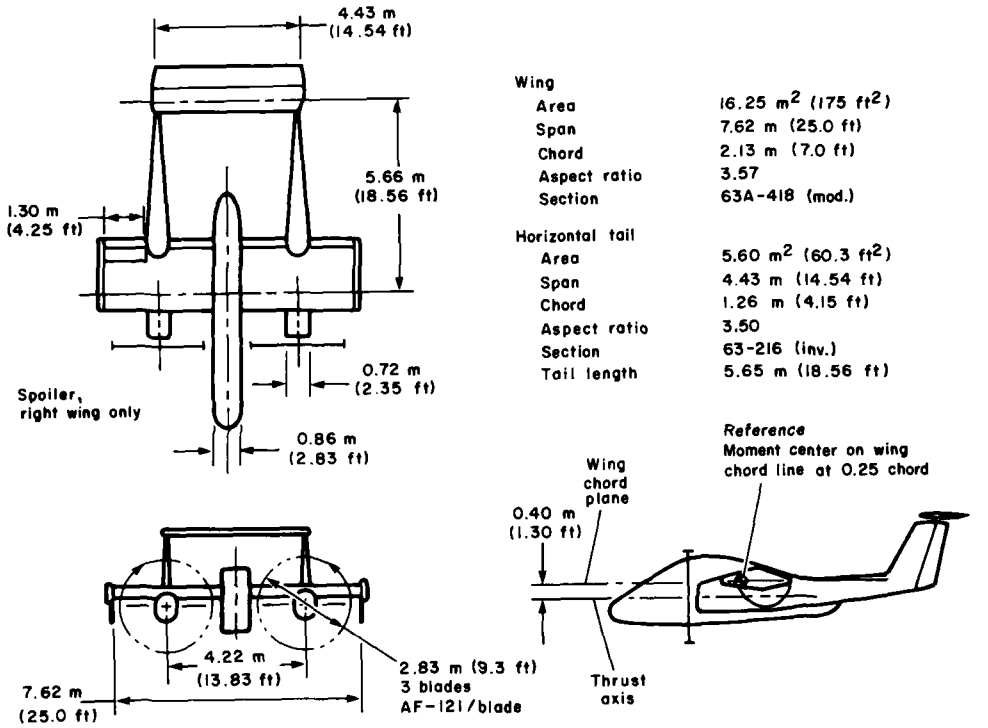

(a) Three view.

Figure 2.– Geometry of model.

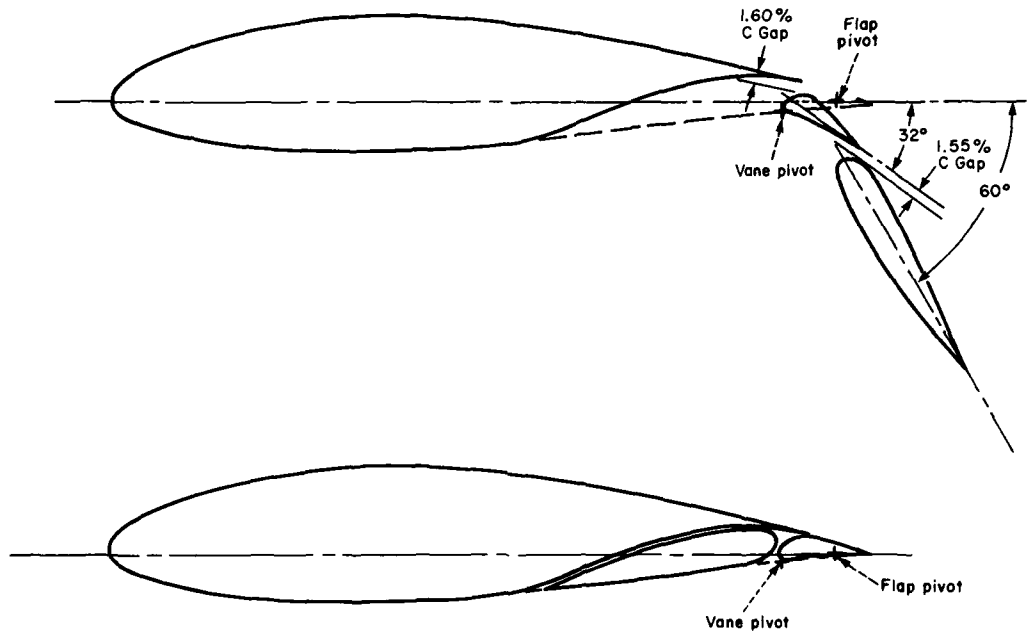

(b) Typical airfoil and flap cross section and arrangement, $\delta_{F/V} = 60/32$ and $\delta_{F/V} = 180/0$.

Figure 2.– Continued.

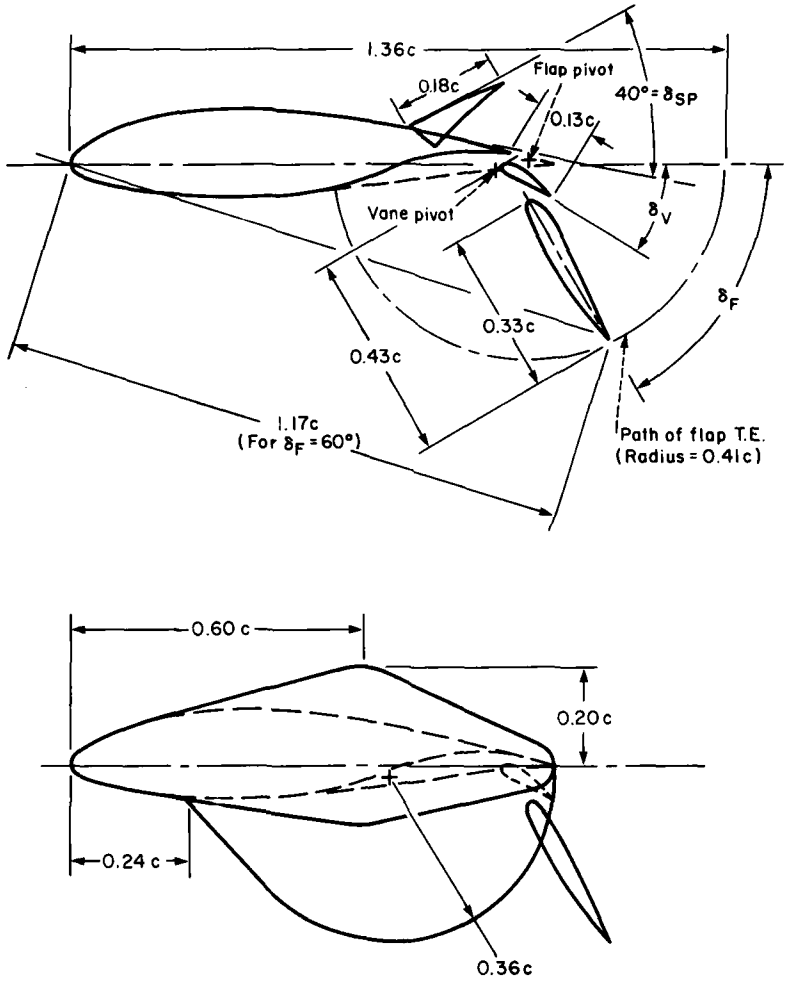

(c) Detail of spoiler and end plate geometry, $\delta_{F/V}$ = 60/32 shown.

Figure 2.– Concluded.

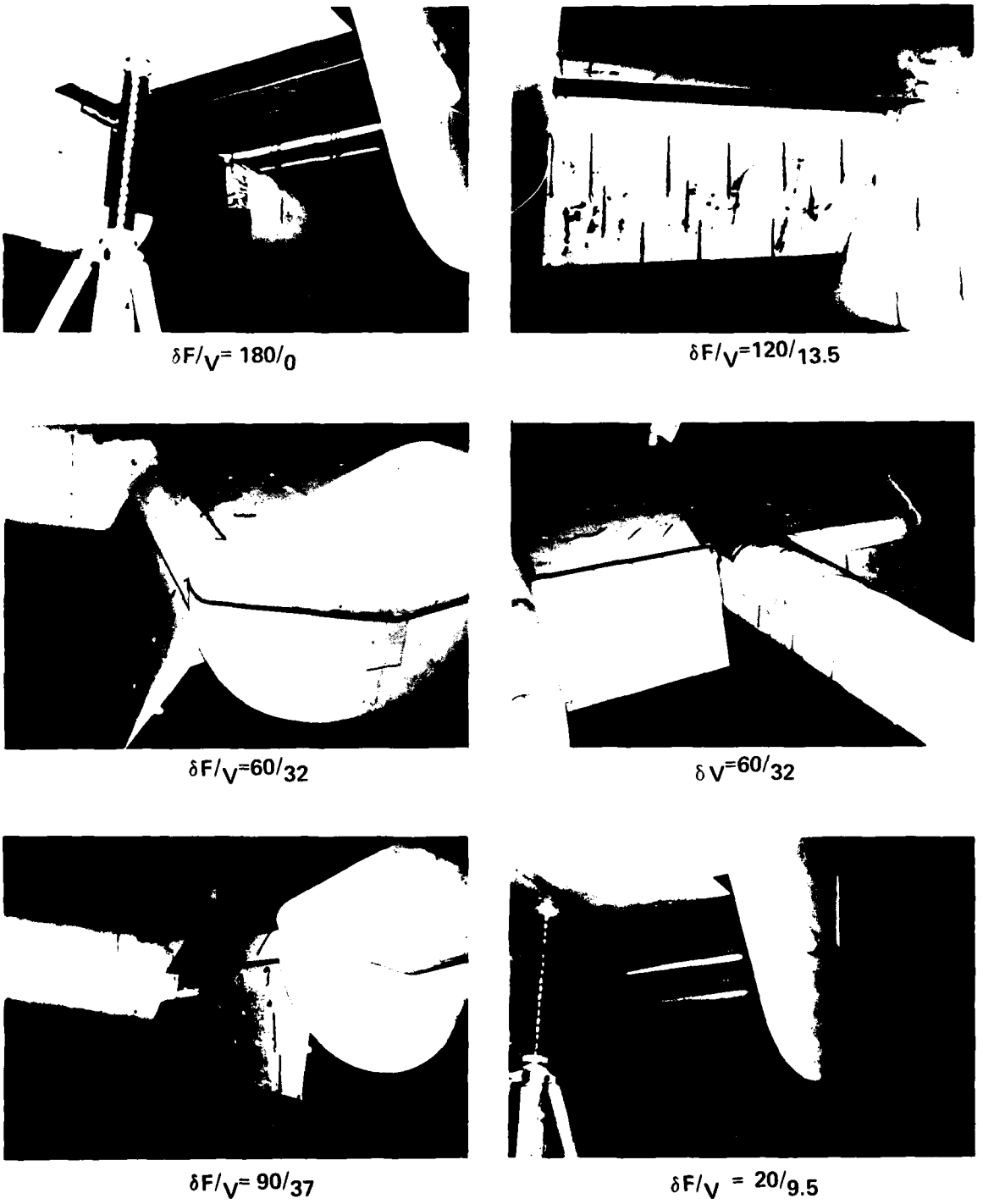

Figure 3. - Photos of several flap deflections.

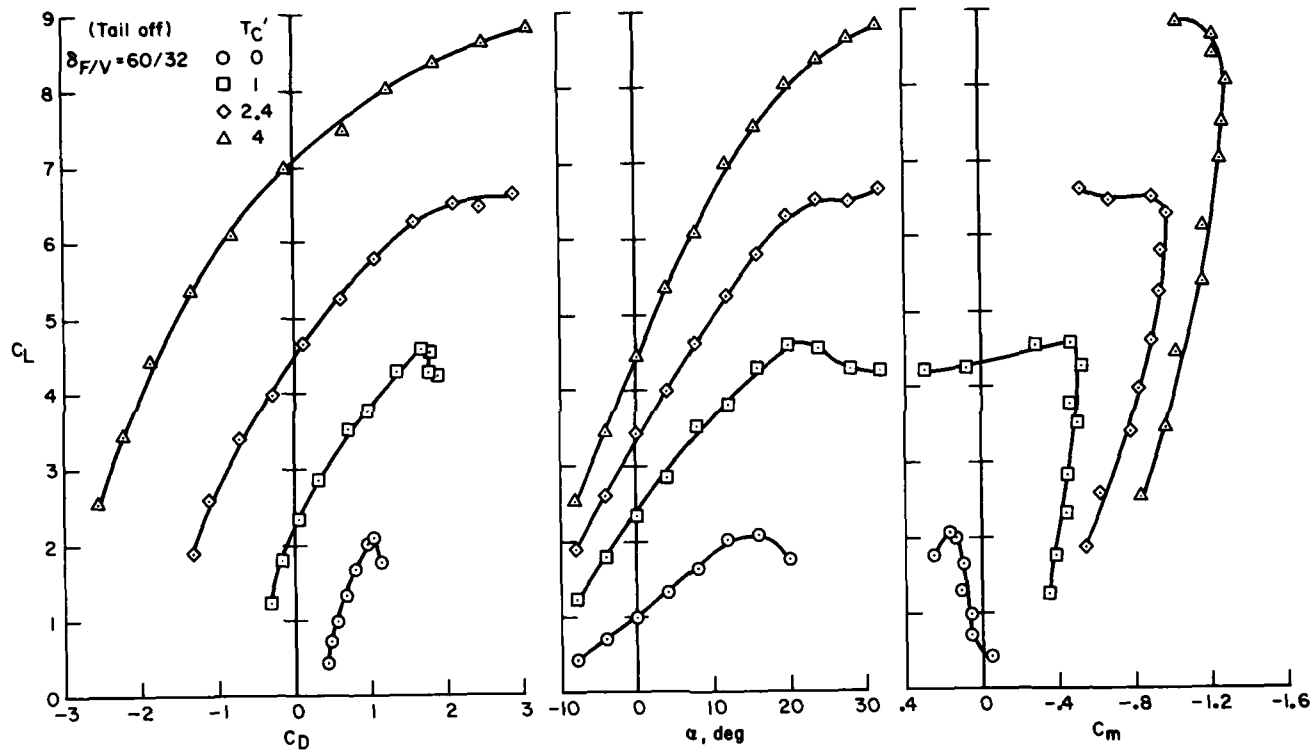

(a) Horizontal tail removed.

Figure 4.– Basic longitudinal data, $\delta_{F/V} = 60/32$.

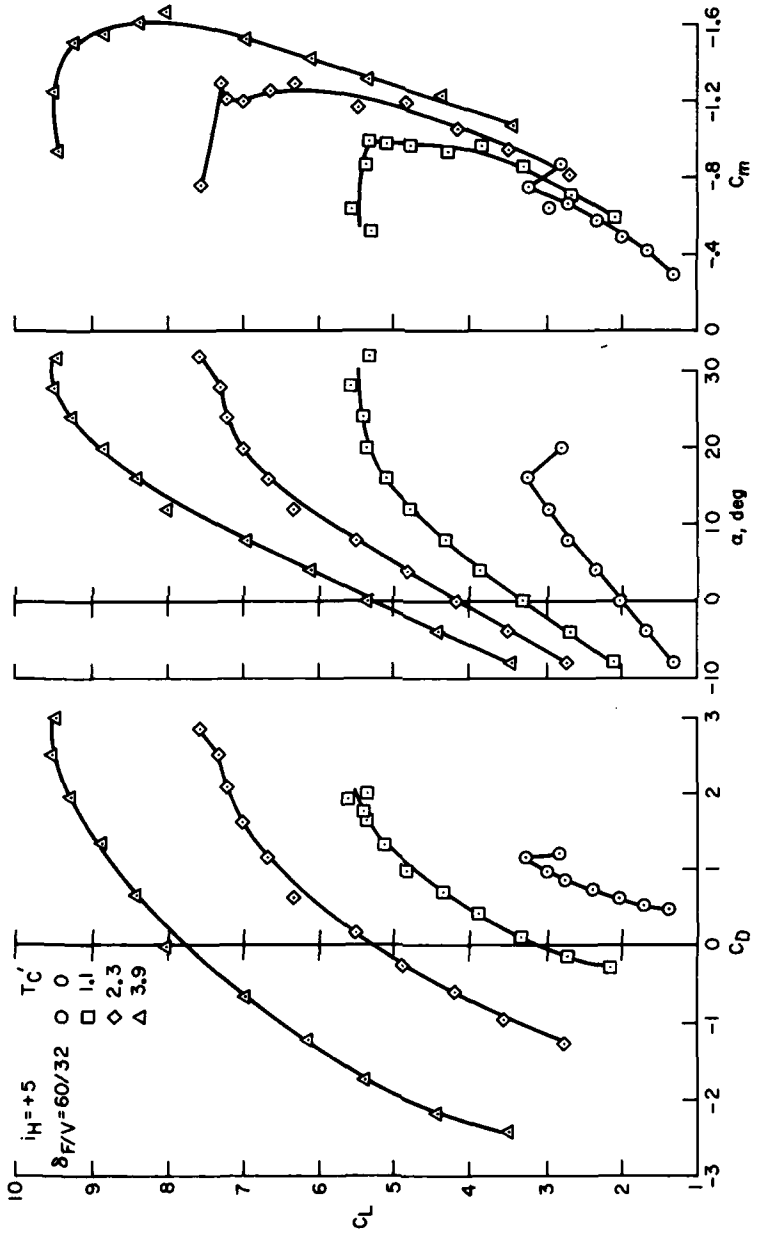

(b) $i_H = +5$.

Figure 4.– Continued.

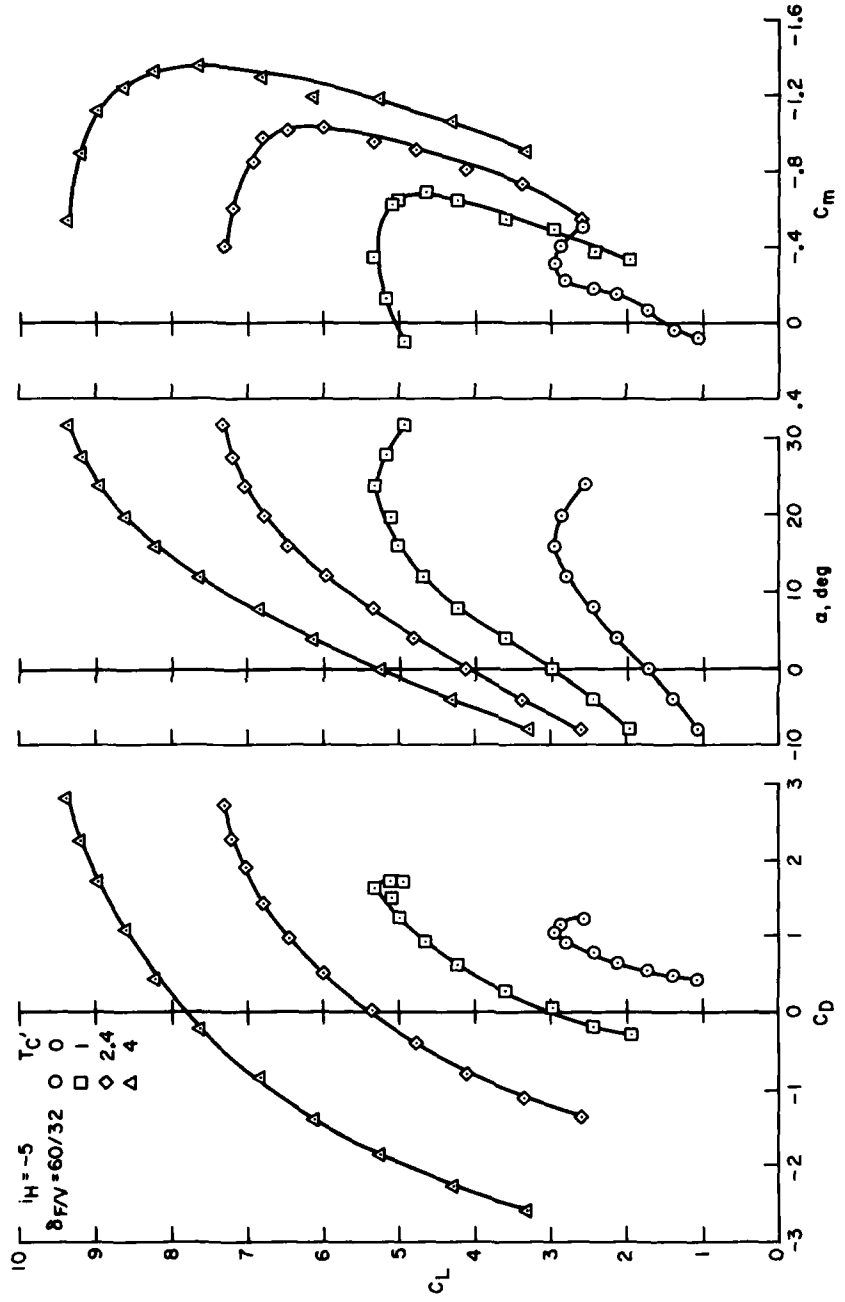

(c) $i_H = -5$.

Figure 4.– Continued.

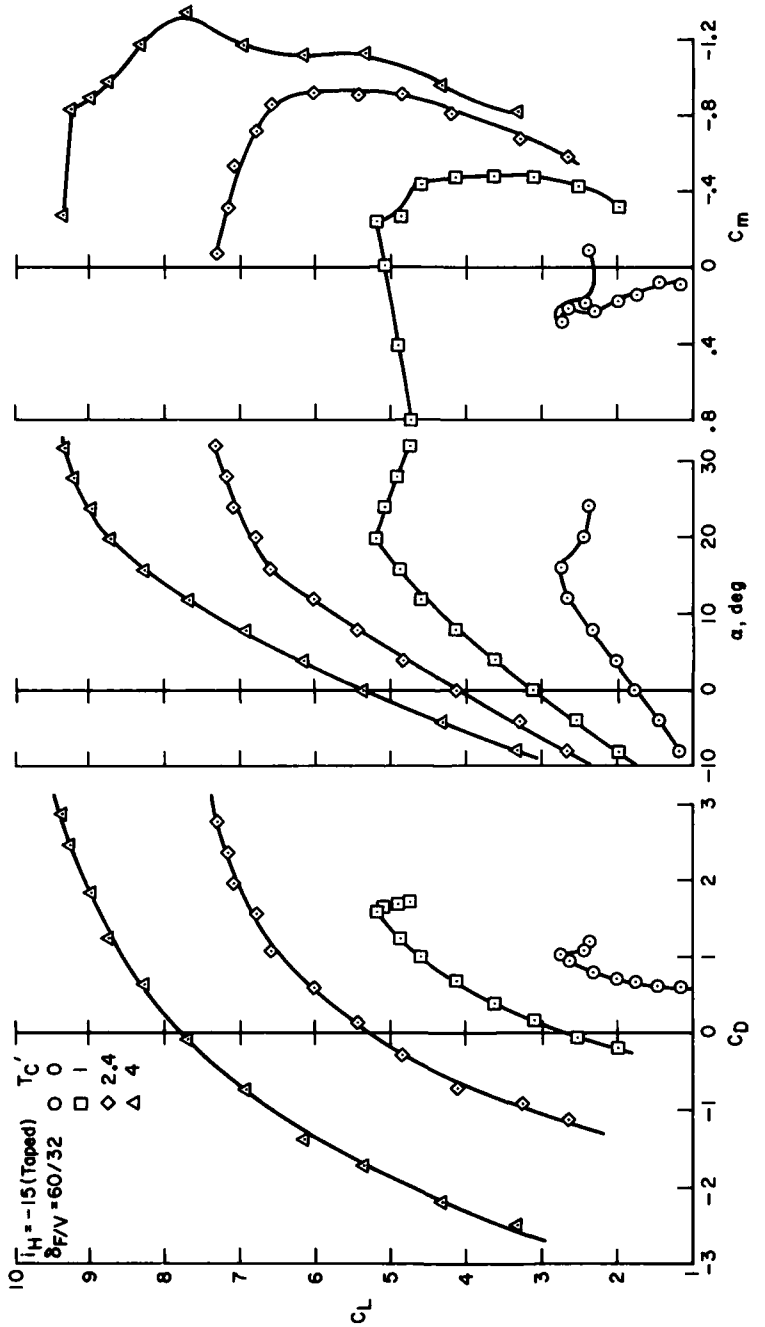

(d) $i_H = -15$ (stabilizer-elevator juncture taped, lower surface).

Figure 4.– Concluded.

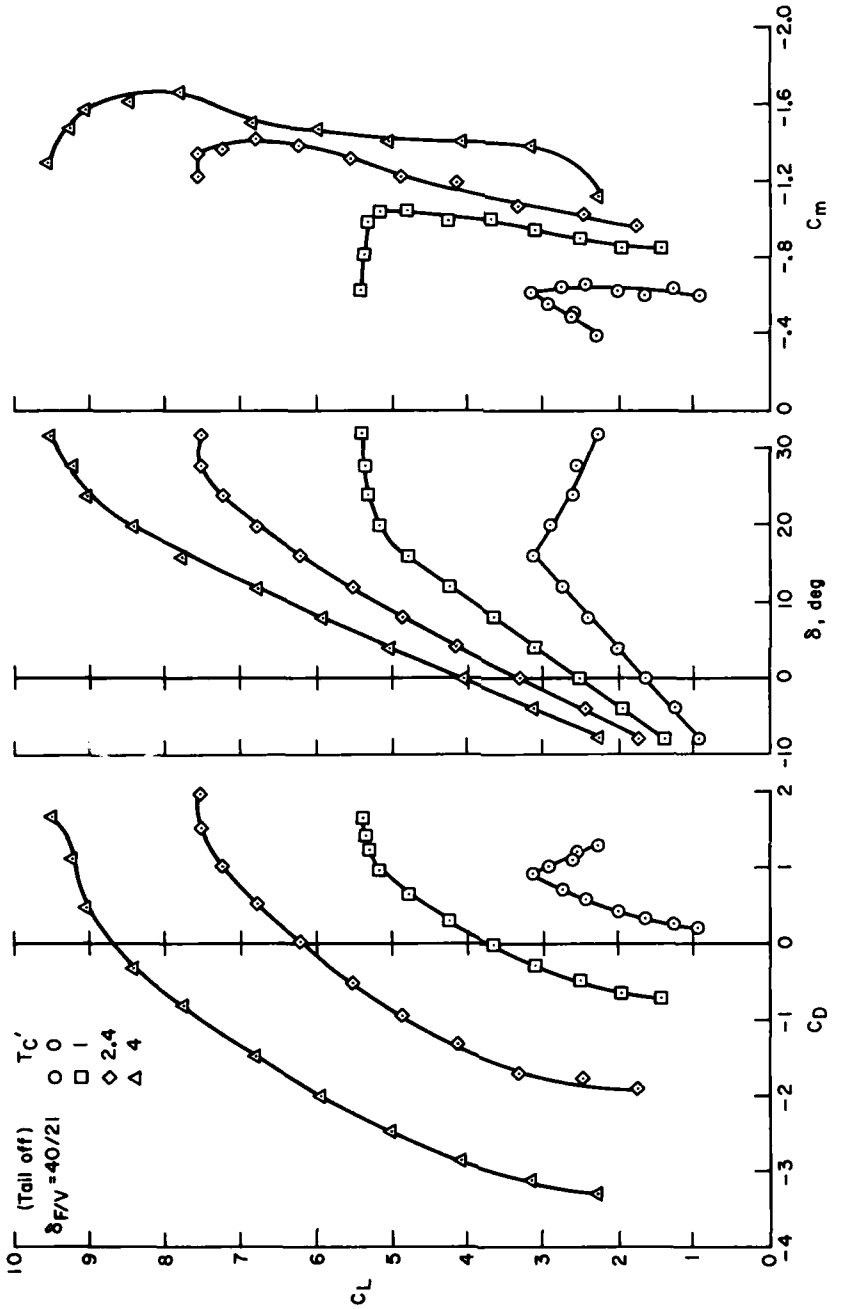

(a) Horizontal tail removed.

Figure 5.– Basic longitudinal data, $\delta_{F/V} = 40/21$.

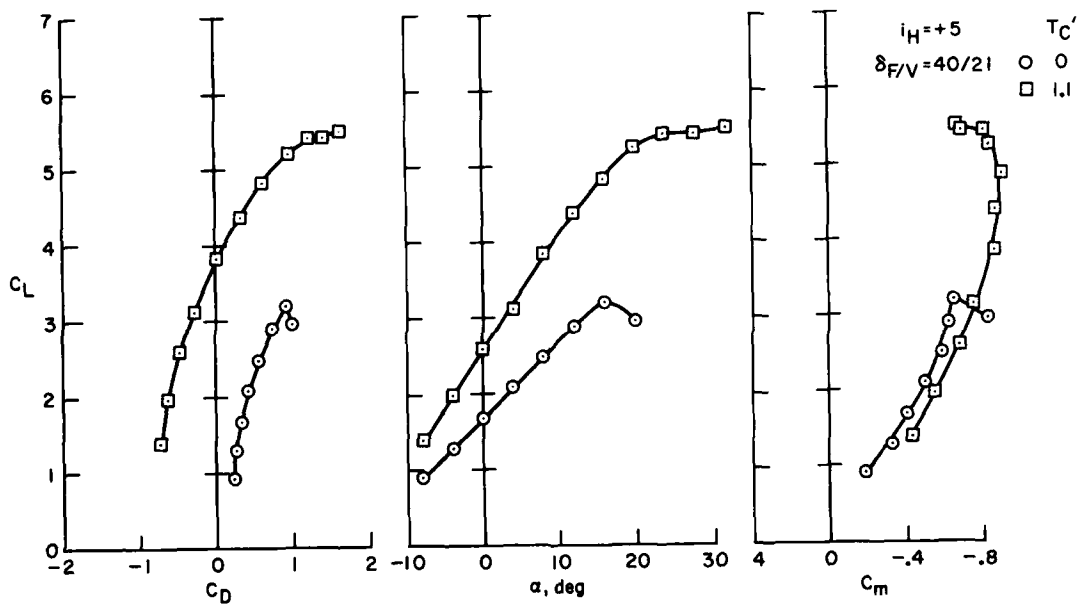

(b) $i_H = +5$.

Figure 5.– Concluded.

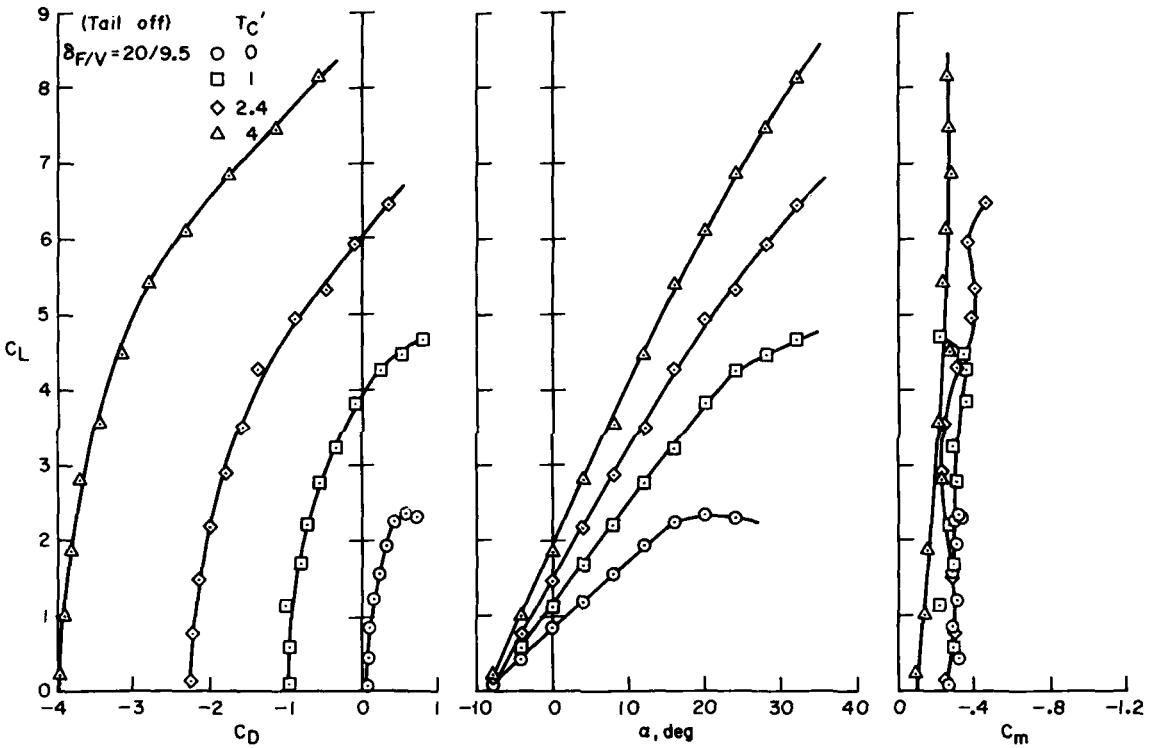

(a) Horizontal tail removed.

Figure 6. Basic longitudinal data, $\delta_{F/V}$ = 20/9.5.

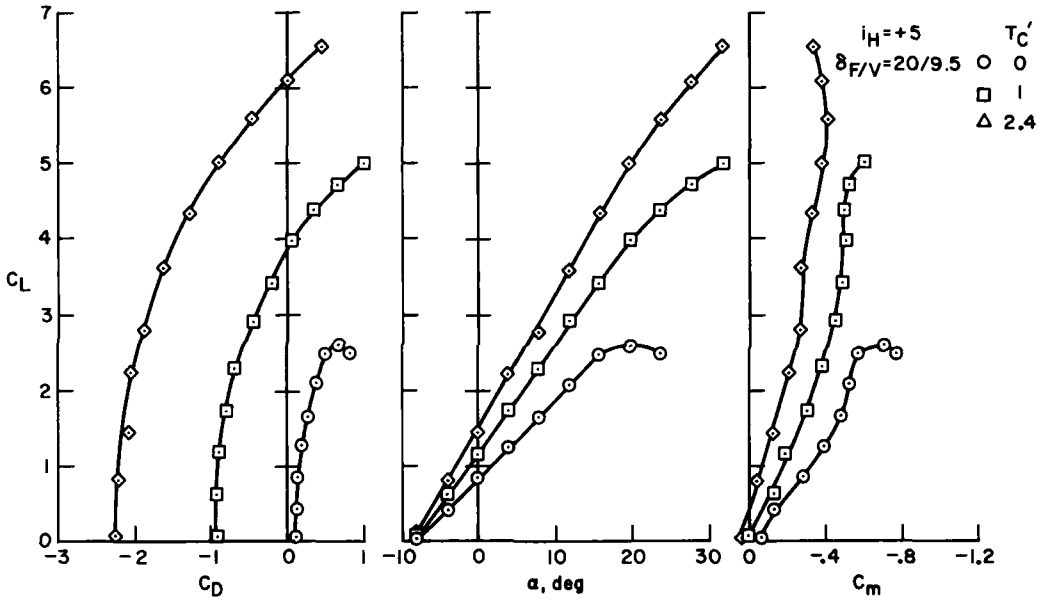

(b) $i_H = +5$.

Figure 6.– Continued.

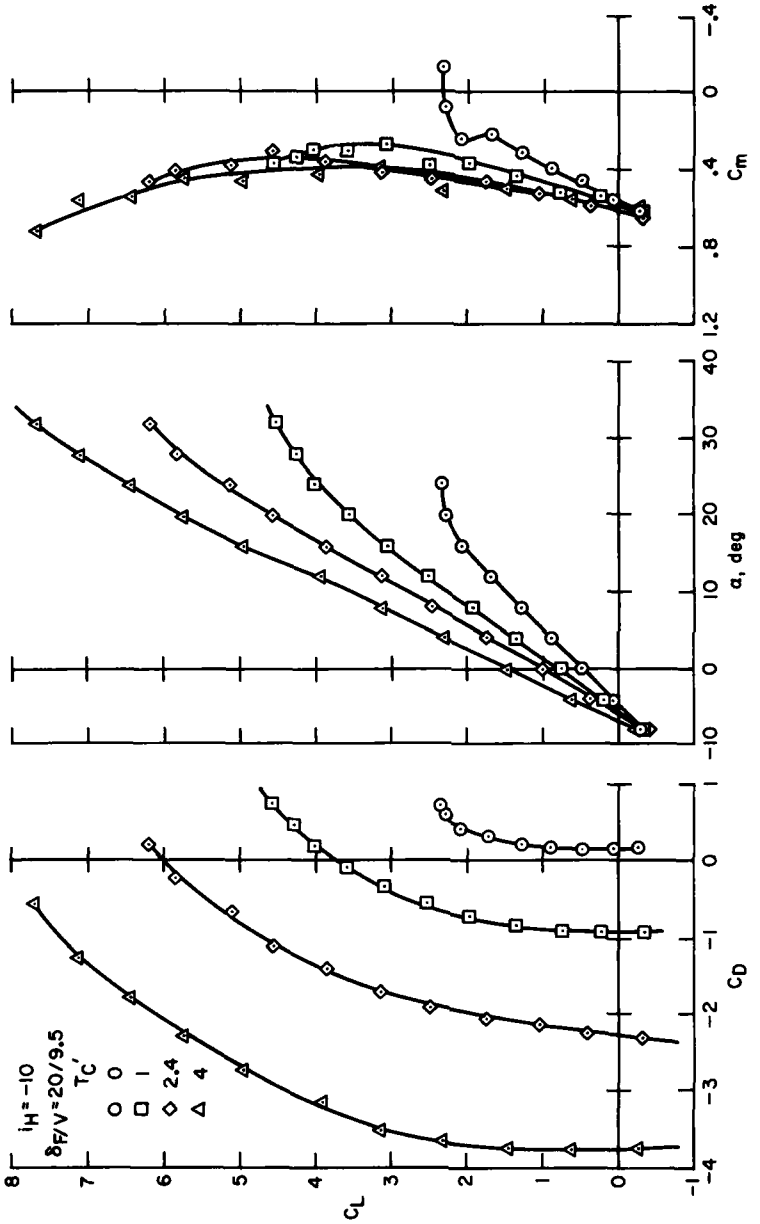

(c) $i_H = -10$.

Figure 6.– Concluded.

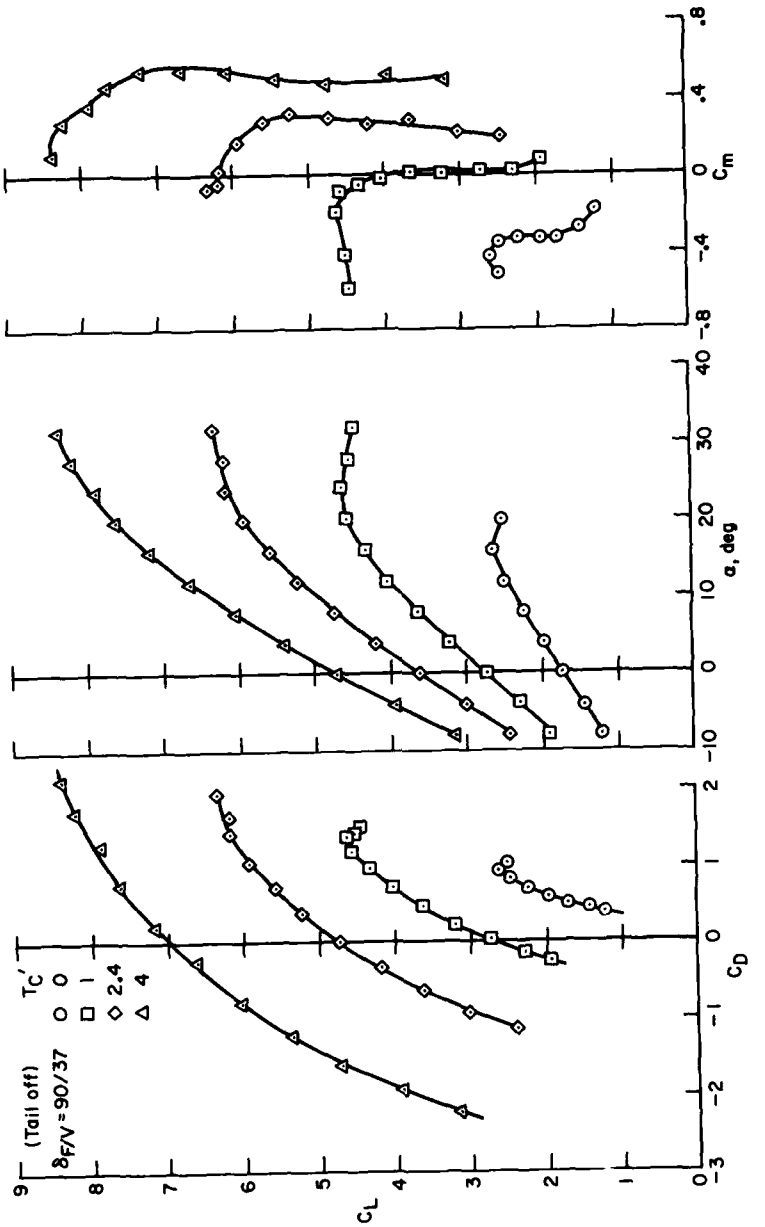

(a) Horizontal tail removed.

Figure 7.– Basic longitudinal data, $\delta_{F/V} = 90/37$.

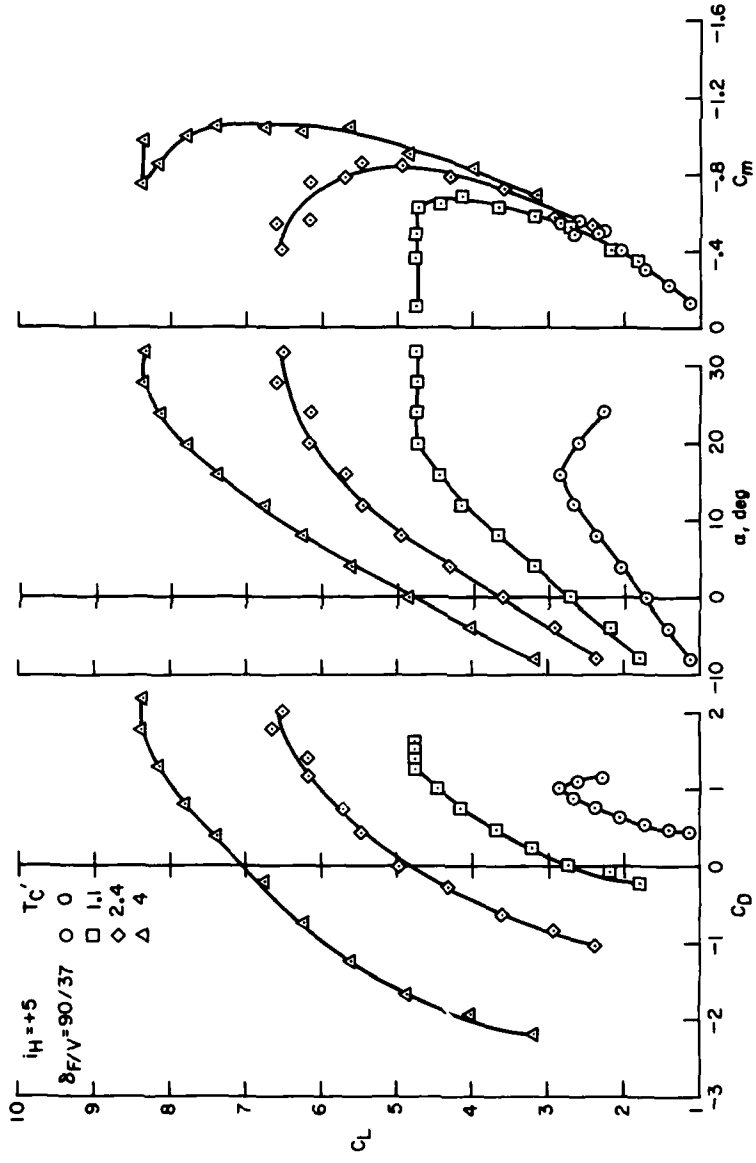

(b) $i_H = +5$.

Figure 7.– Continued.

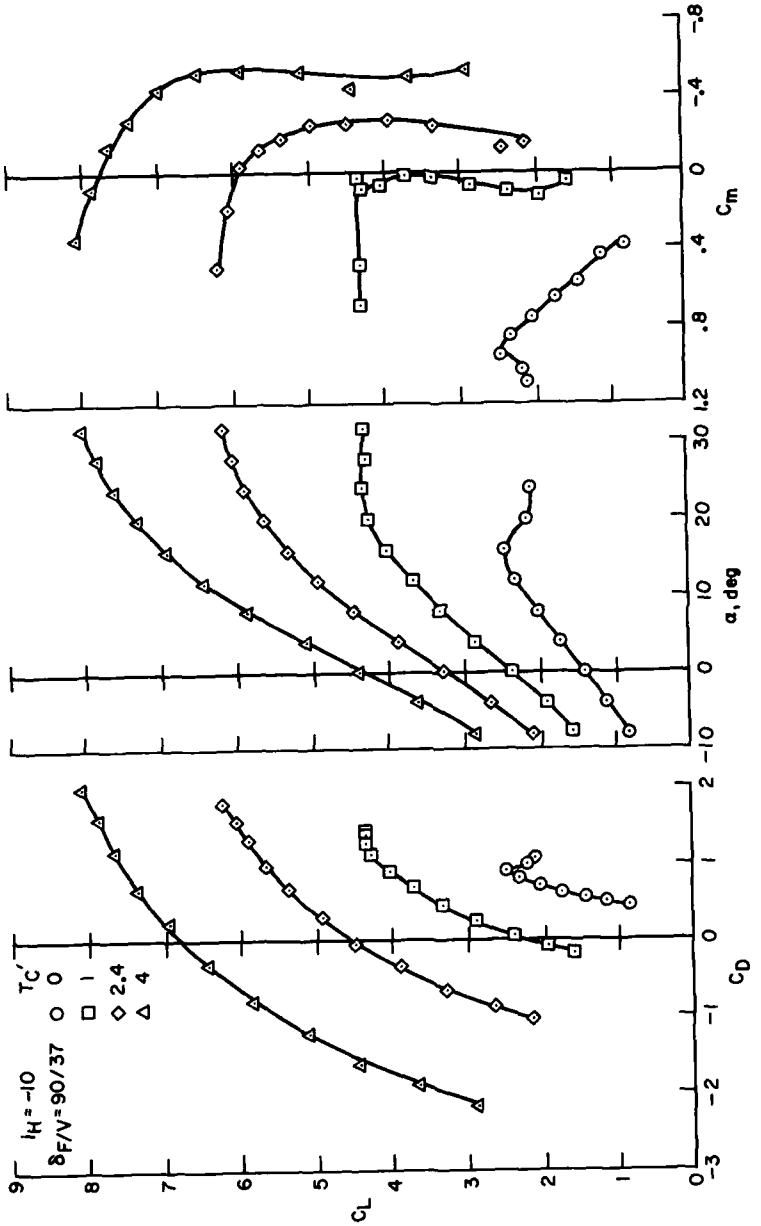

(c) $i_H = -10$.

Figure 7.– Concluded.

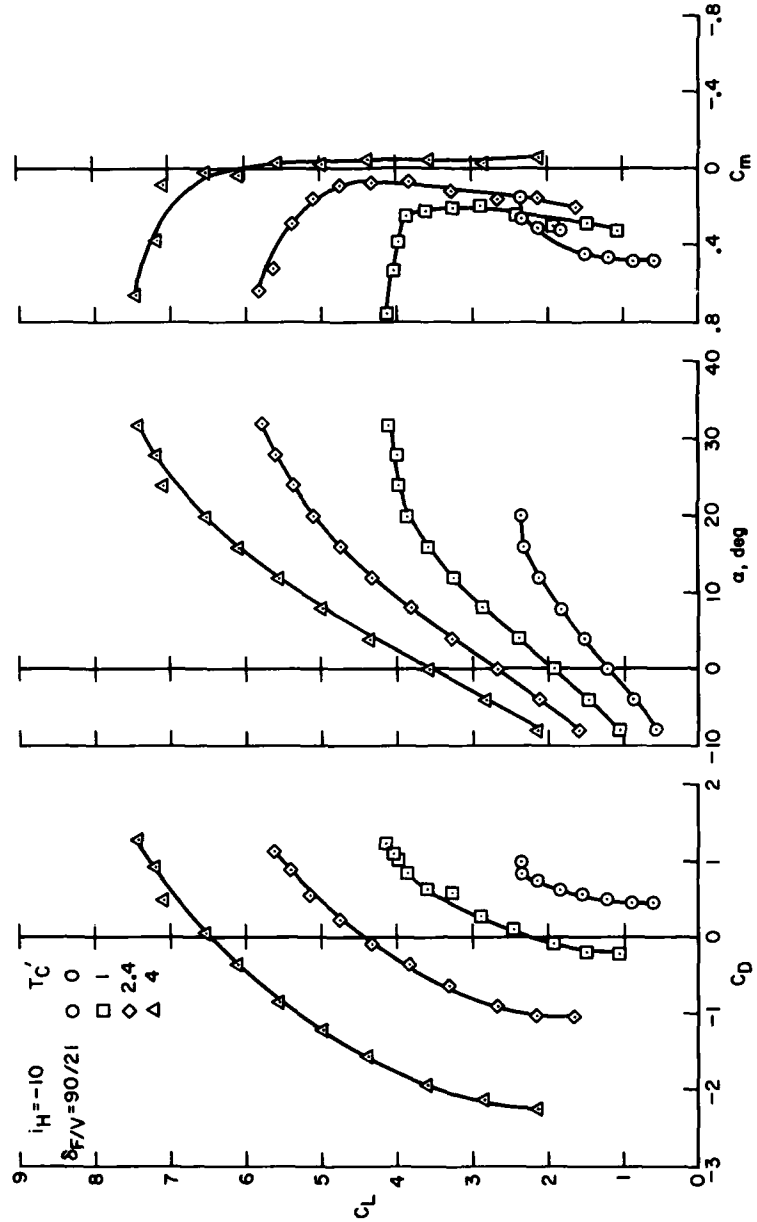

Figure 8.– Basic Longitudinal data, $\delta_{F/V} = 90/21$; $i_H = -10$.

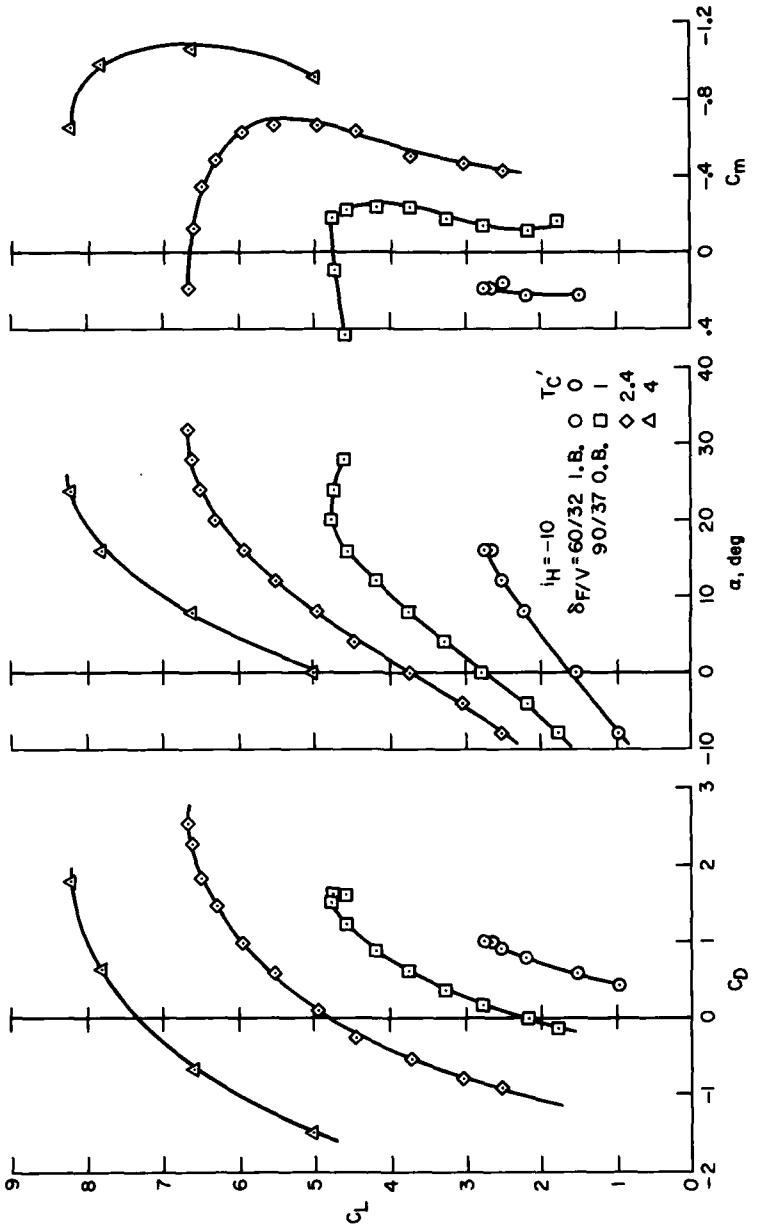

Figure 9.– Basic longitudinal data, $\delta_{F/V} = 60/32$ inboard, 90/37 outboard; $i_H = -10$.

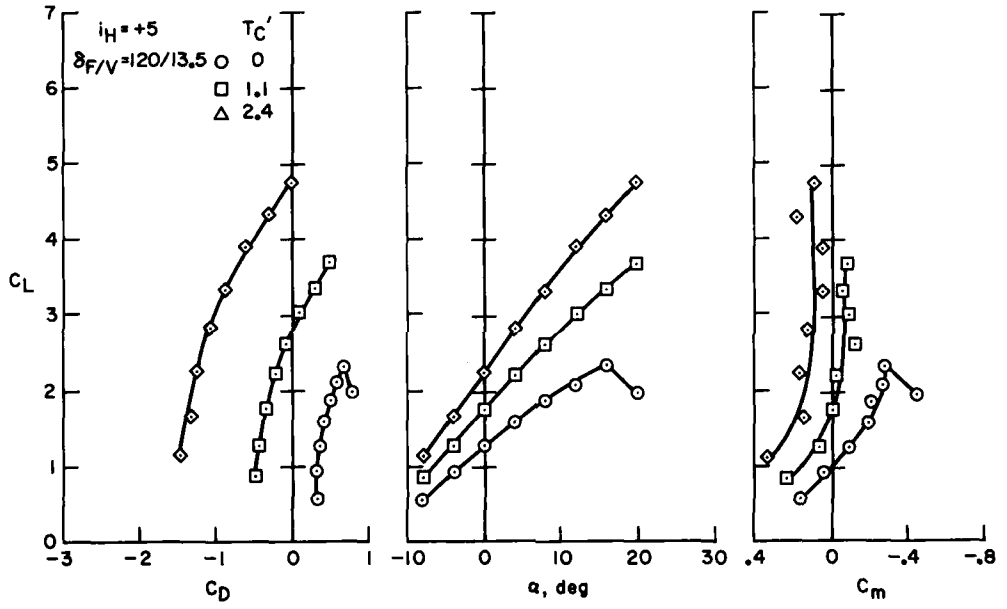

Figure 10.– Basic longitudinal data, $\delta_{F/V} = 120/13.5$; $i_H = +5$.

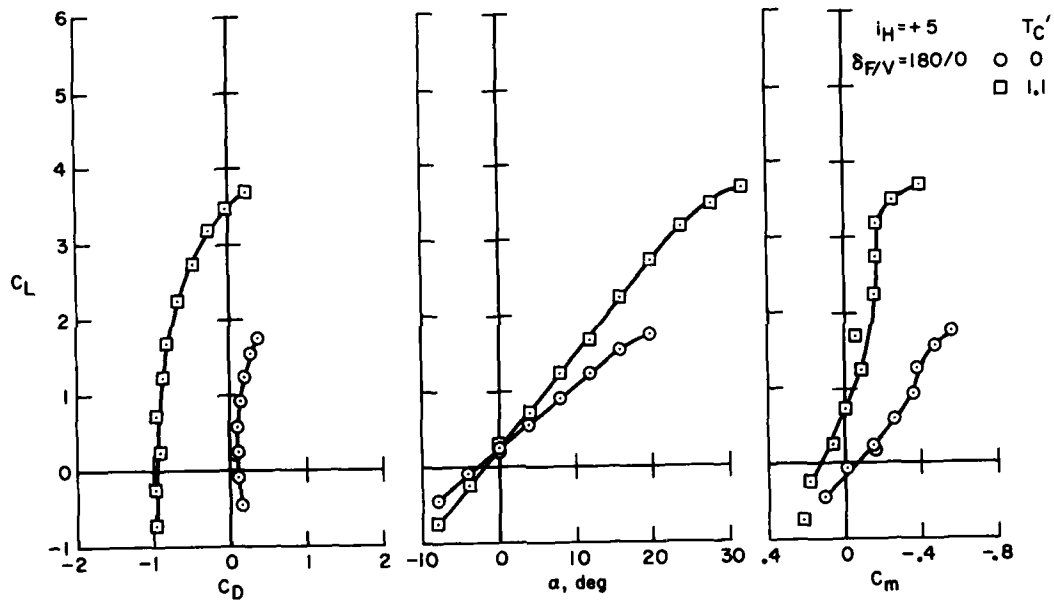

Figure 11.– Basic longitudinal data, $\delta_{F/V}$ = 180/0 (flap stored); i_H = +5.

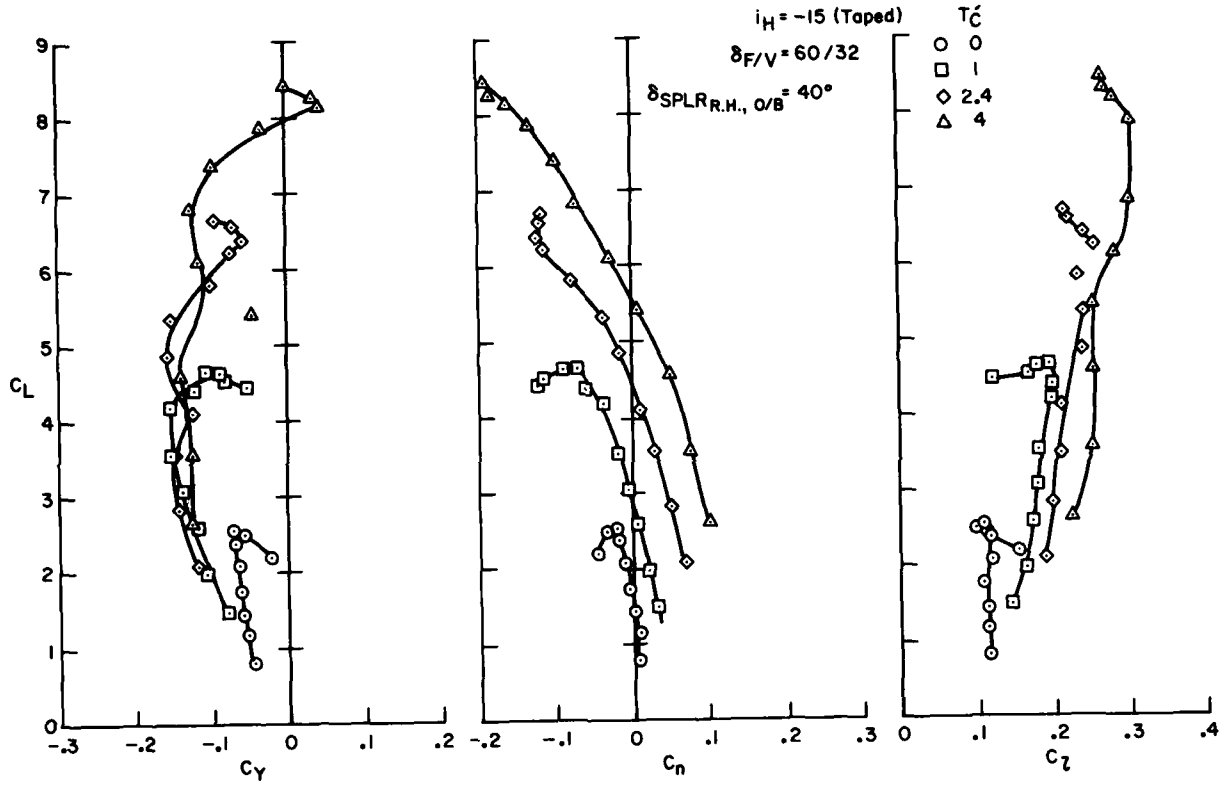

(a) $\delta_{F/V} = 60/32$; $i_H = -15$, taped.

Figure 12.– Lateral control effectiveness; spoiler deflected 40°, right hand outboard section.

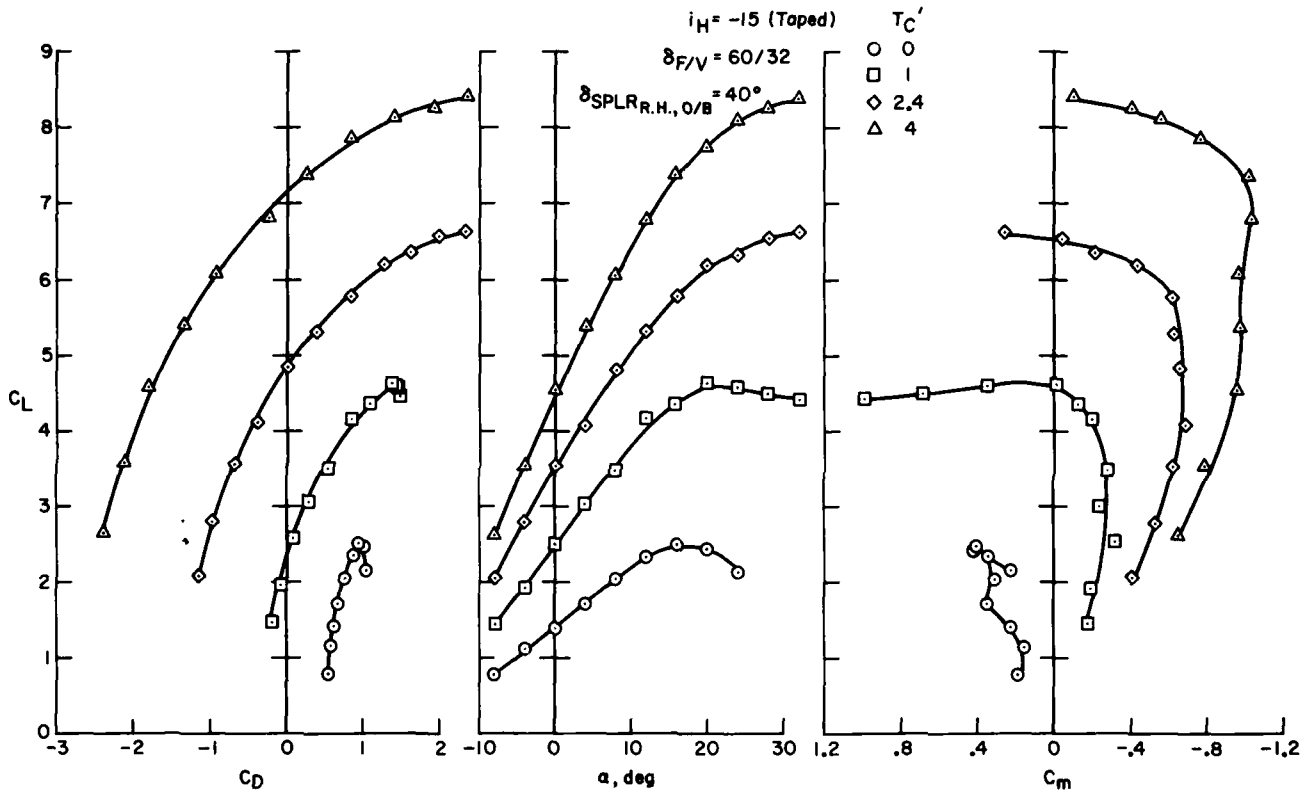

(a) Concluded.

Figure 12.– Continued.

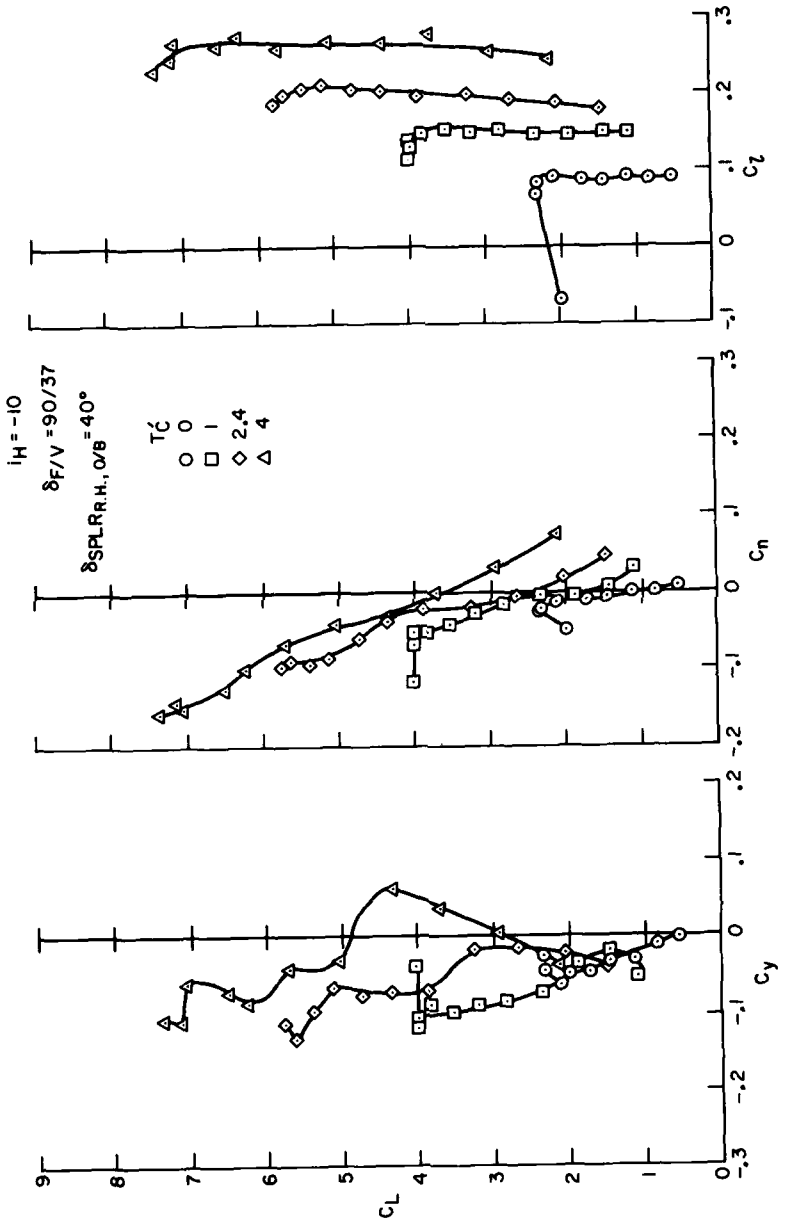

(b) $\delta_{F/V} = 90/32; i_H = -10$.

Figure 12.– Continued.

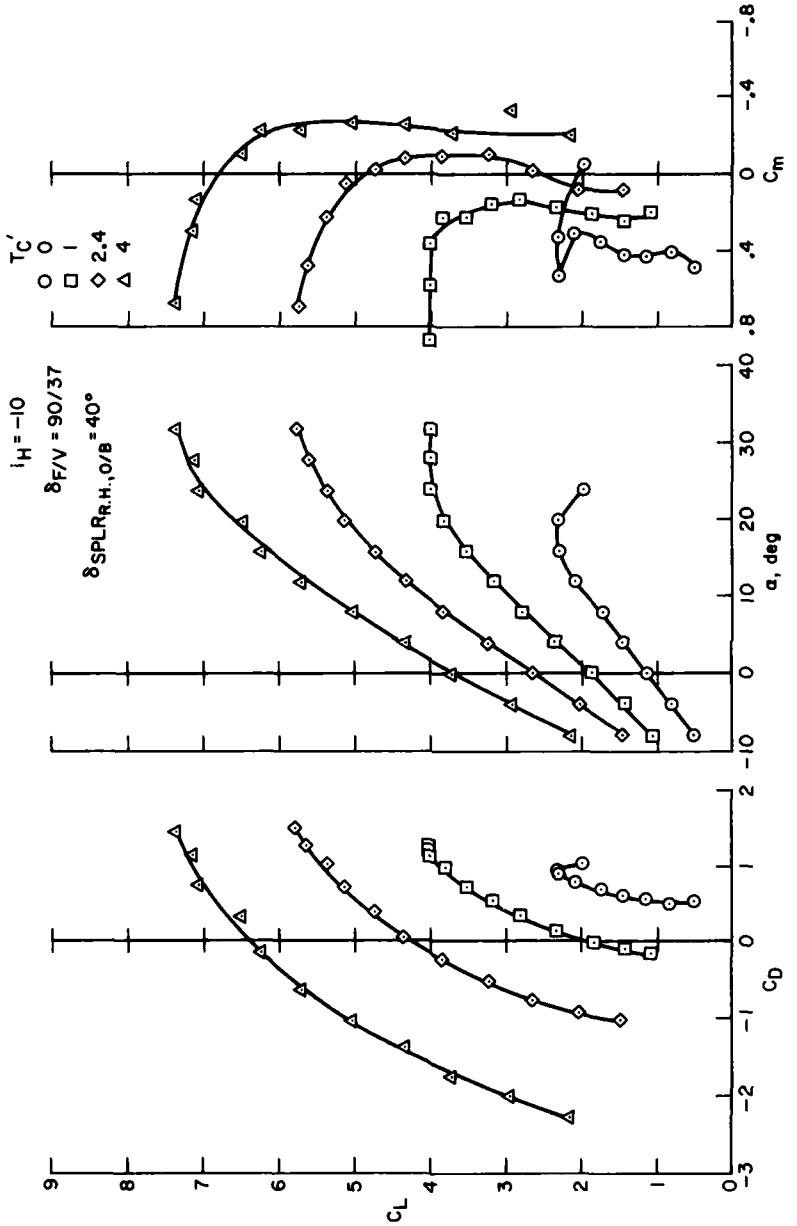

(b) Concluded.

Figure 12.– Concluded.

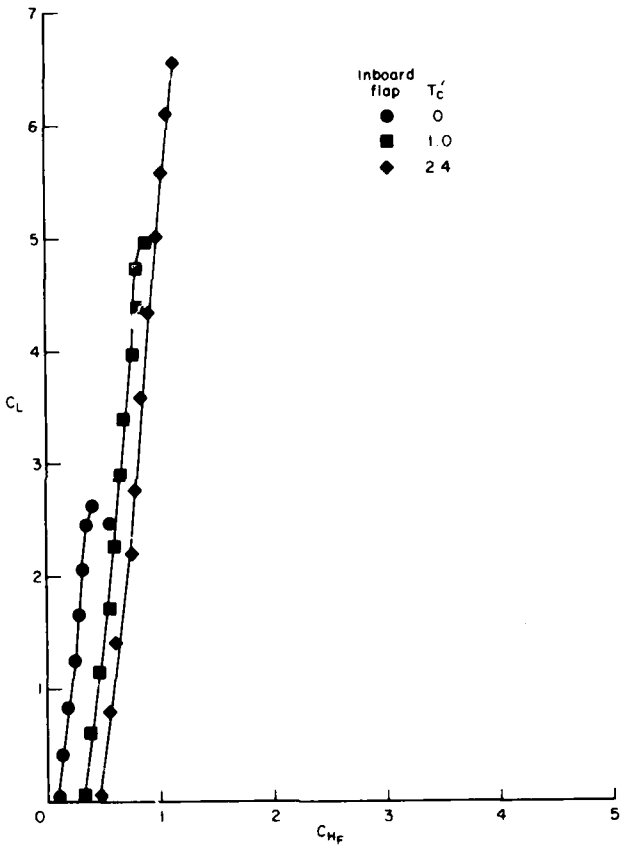

(a) $\delta_{F/V} = 20/9.5$.

Figure 13.– Flap hinge moment data, right wing.

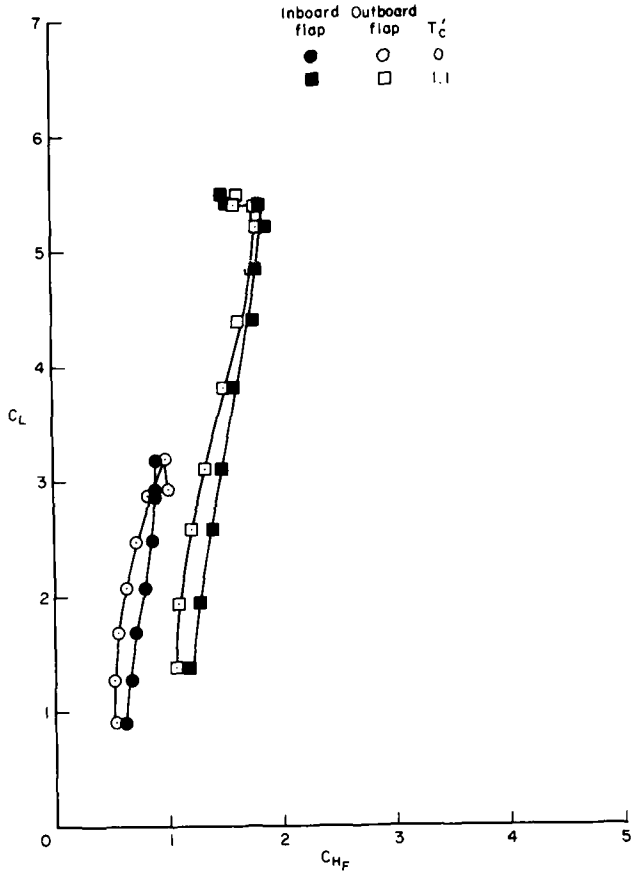

(b) $\delta_{F/V} = 40/21$.

Figure 13.– Continued.

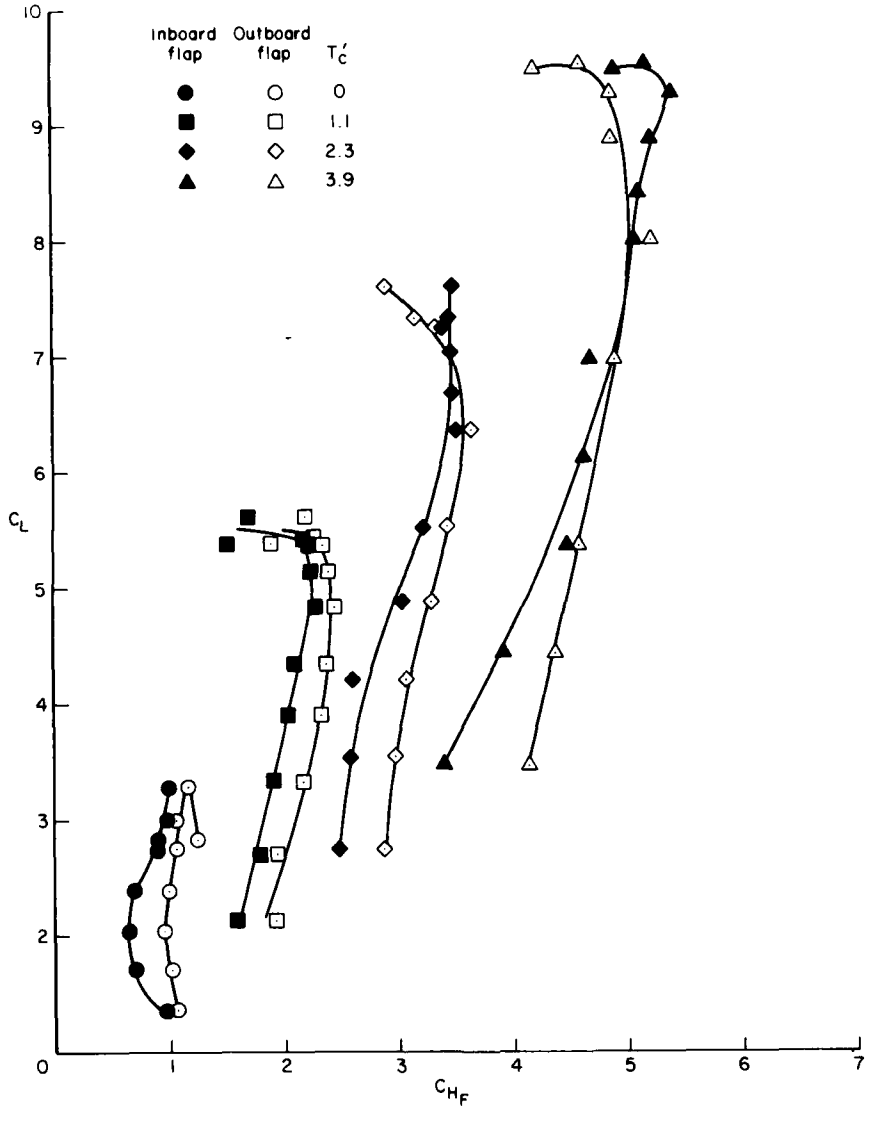

(c) $\delta_{F/V} = 60/32$.

Figure 13.– Continued.

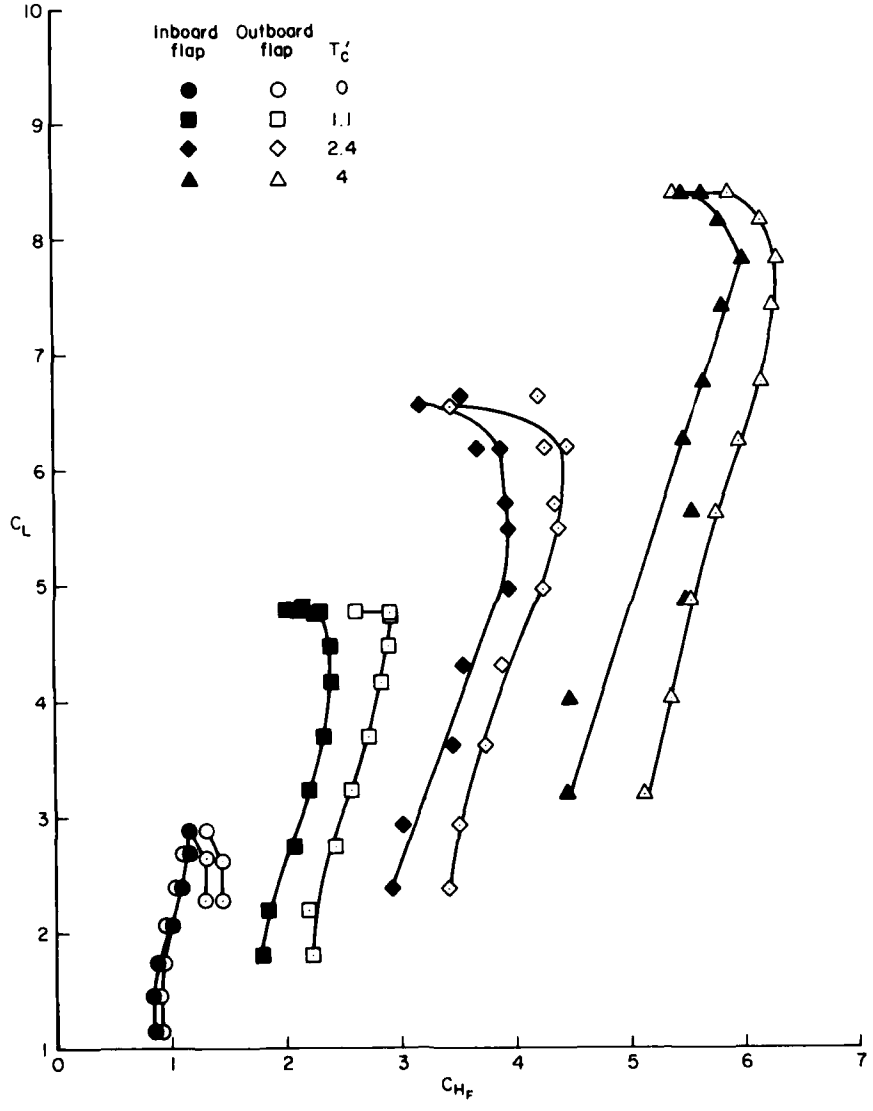

(d) $\delta_{F/V} = 90/37$.

Figure 13.– Continued.

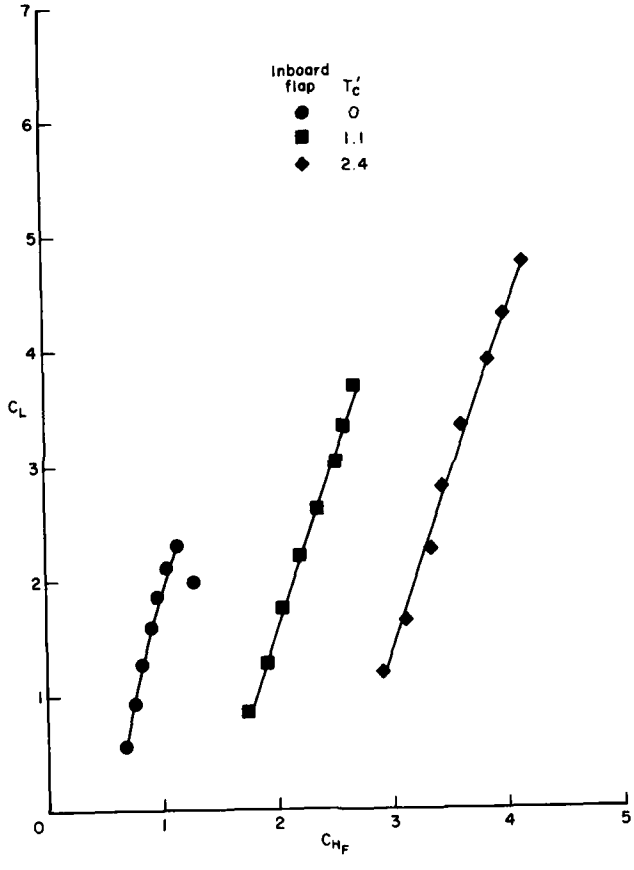

(e) $\delta_{F/V} = 120;13.5$.

Figure 13.– Concluded.

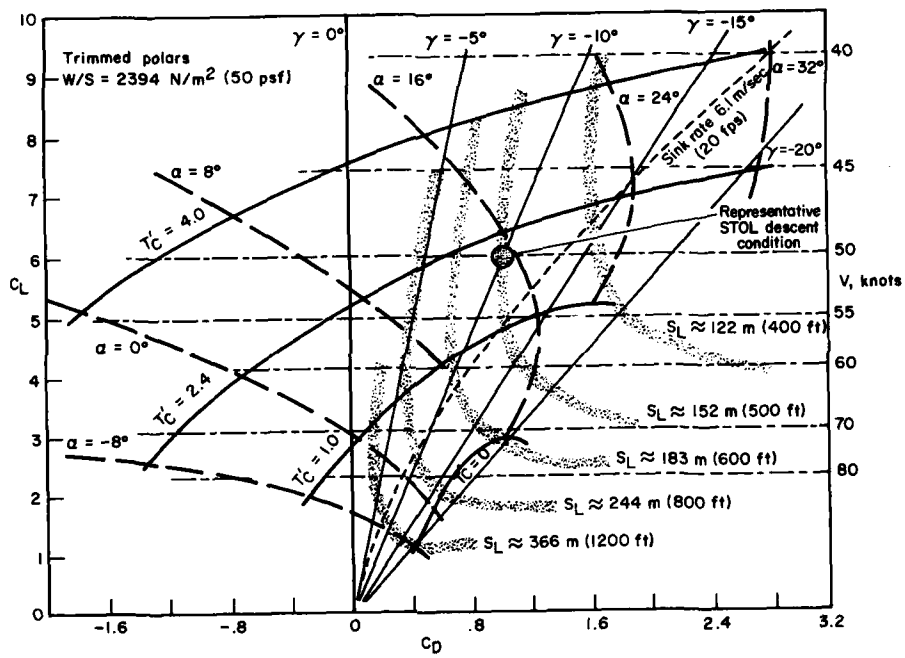

Figure 14.– Trimmed polars with $\delta_{F/V} = 60/32$ for STOL utility aircraft – showing representative landing approach parameters.

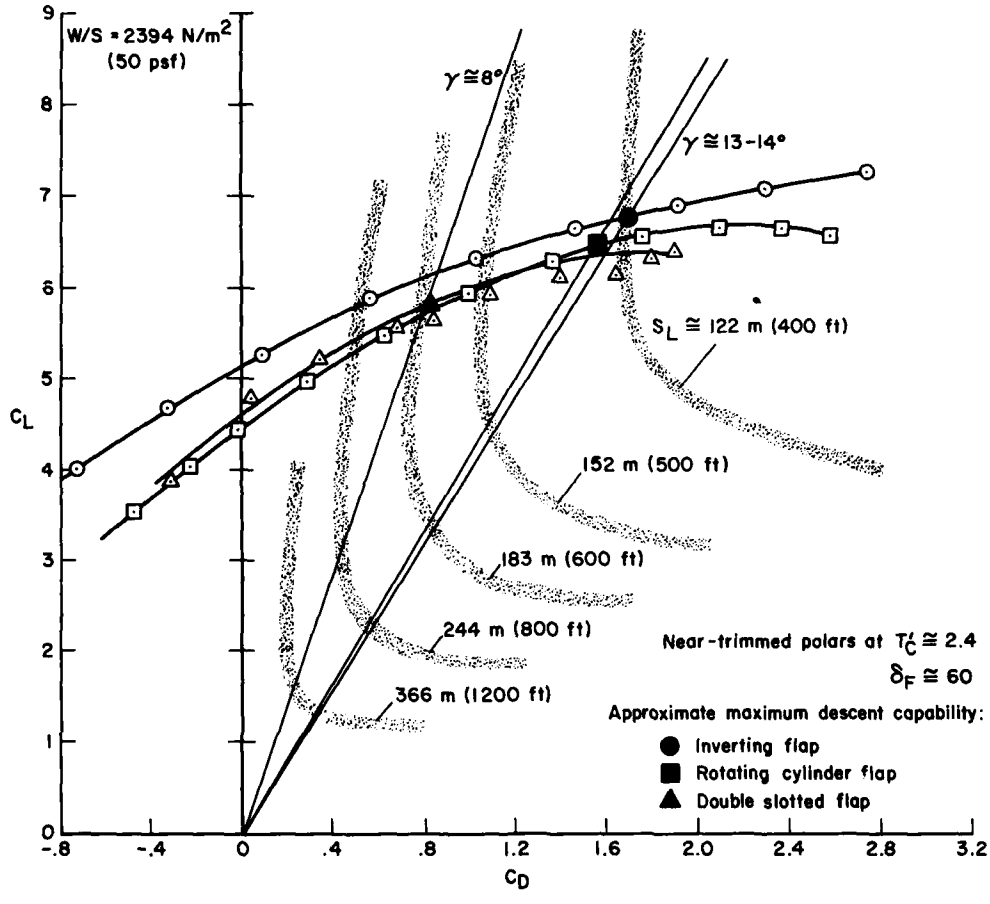

Figure 15.– Landing approach condition, descent capability comparison – three different flap systems.

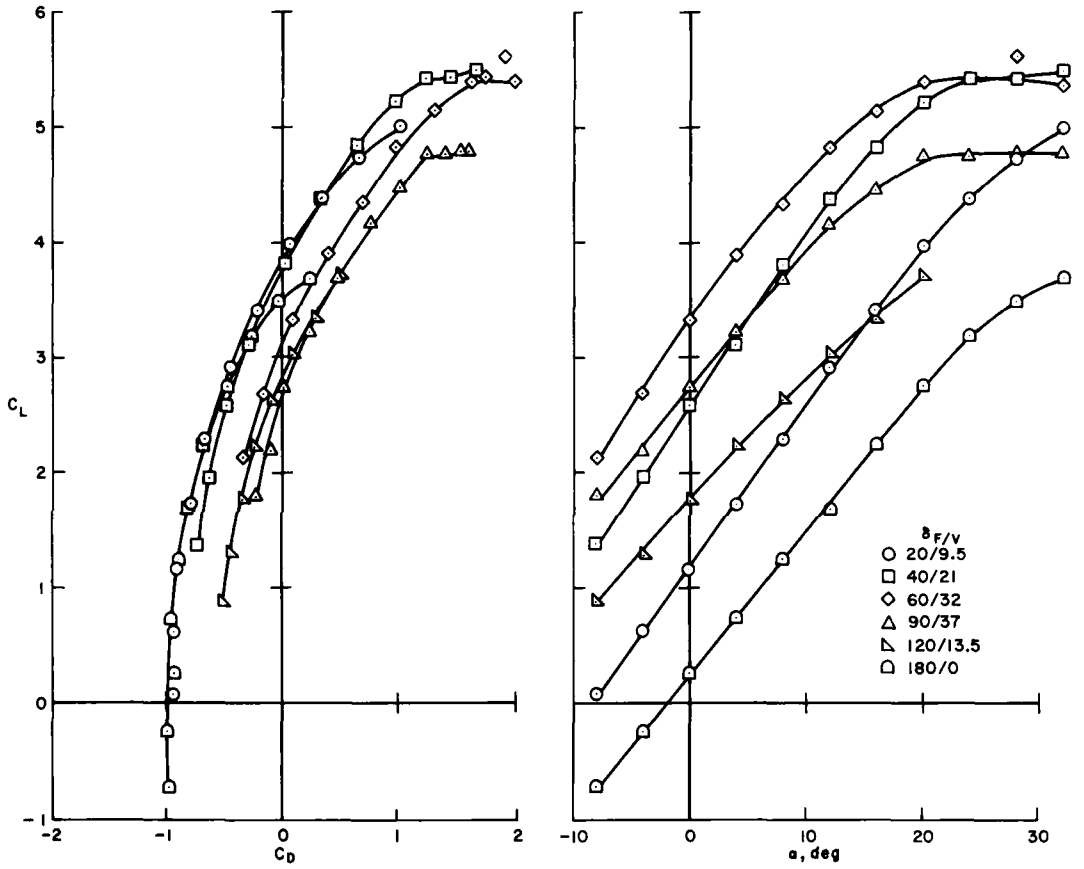

(a) Lift and drag data, cg at 0.25 $\bar{c}$, on chord line.

Figure 16.– Summary of T'_C = 1 longitudinal data for a range of flap settings.

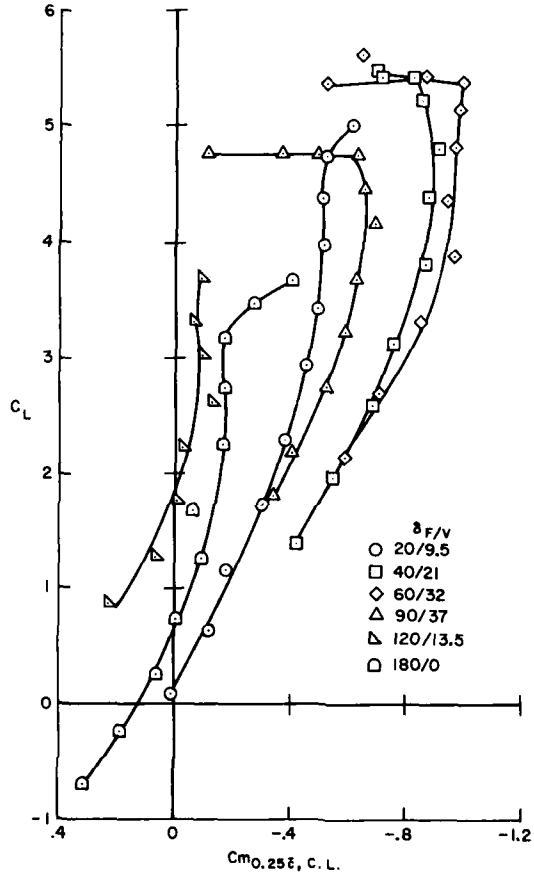

(b) Pitching-moment data, cg at 0.25 $\bar{c}$, on chord line.

Figure 16.– Continued.

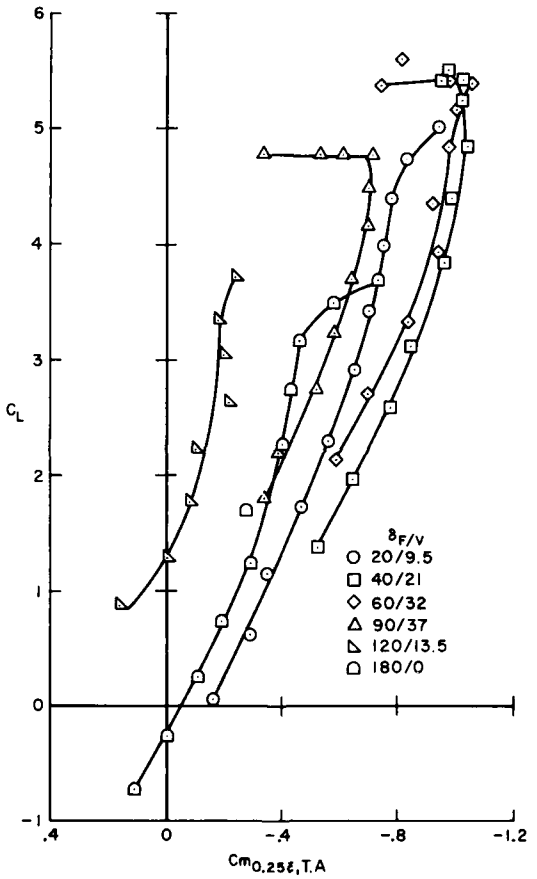

(c) Pitching-moment data, cg at 0.25 $\bar{c}$, on thrust line.

Figure 16.– Concluded.

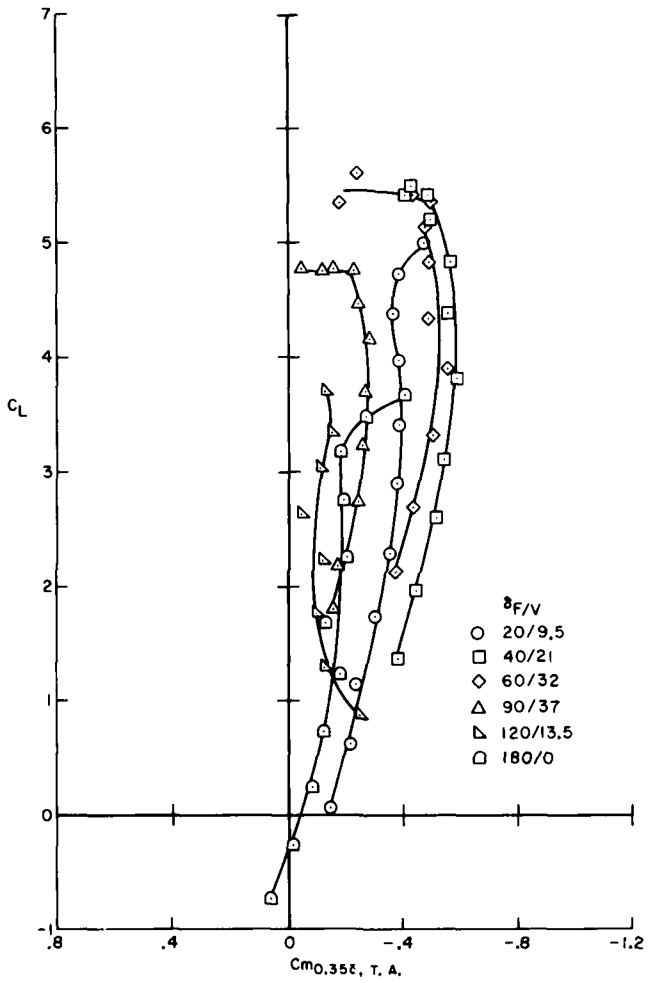

(a) Superposition of $T'_c = 1$ data for a range of flap settings, $i_H = +5°$.

Figure 17.– Pitching-moment data replotted for cg at 0.35 c on the thrust line.

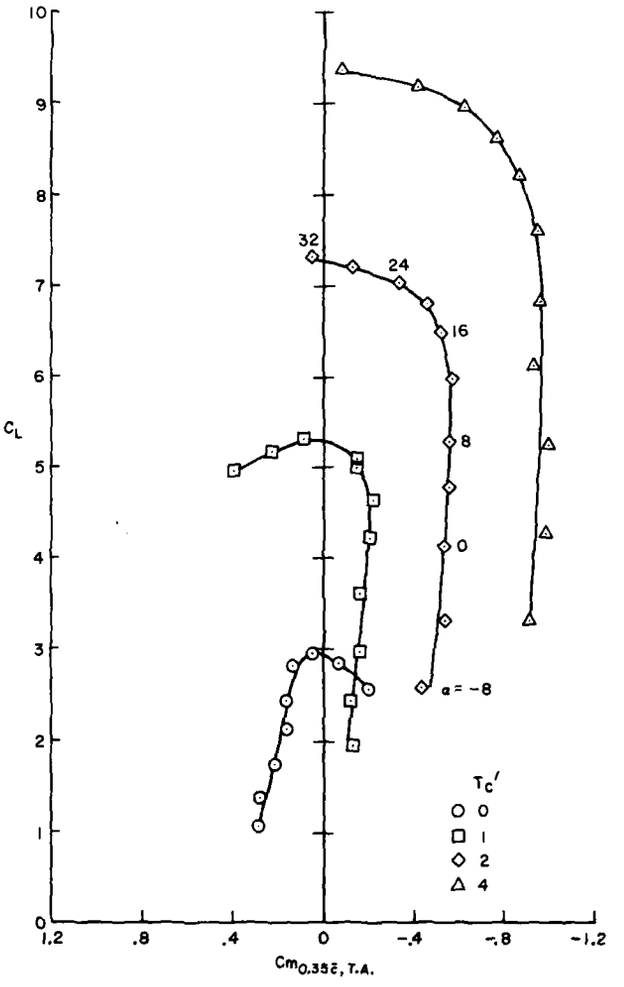

(b) $\delta_{F/V} = 60/32$, $i_H = -5$.

Figure 17.– Continued.

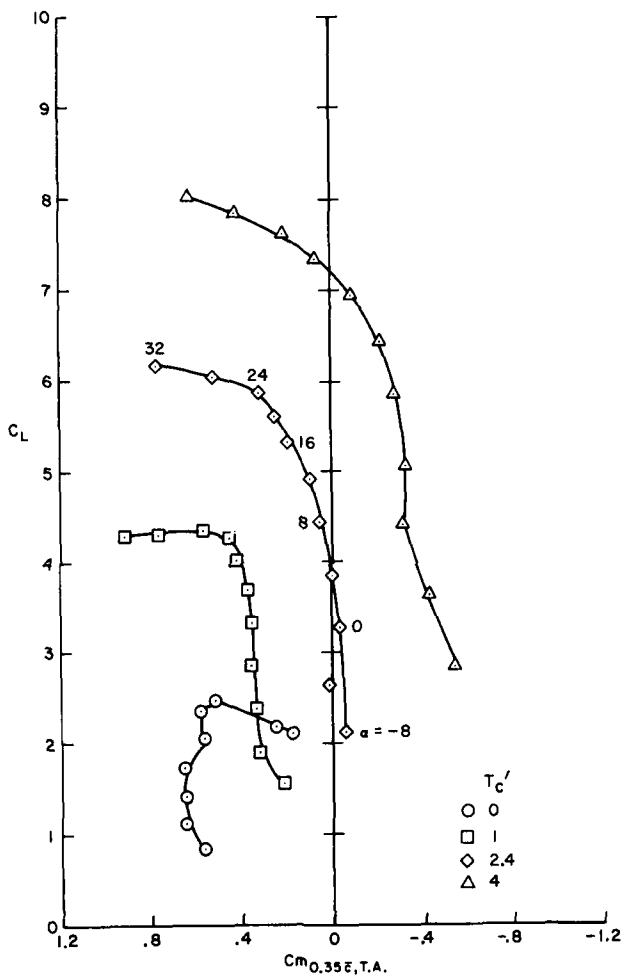

(c) $\delta_{F/V} = 90/32, i_H = -10.$

Figure 17.– Continued.

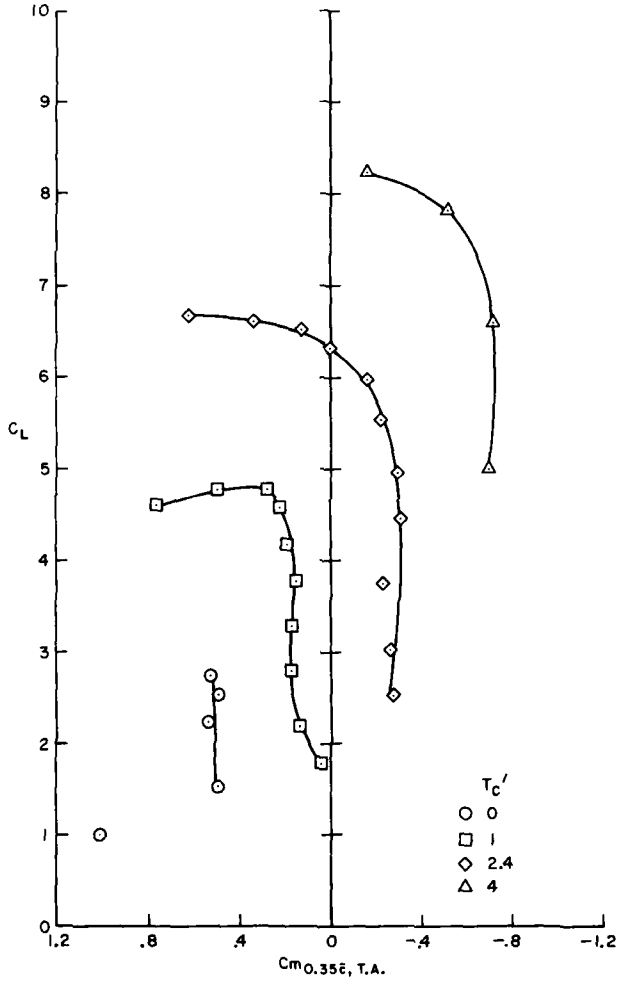

(d) $\delta_{F/V}$ = 60/32 I./B., 90/32 O./B.; i_H = -10.

Figure 17.– Continued.

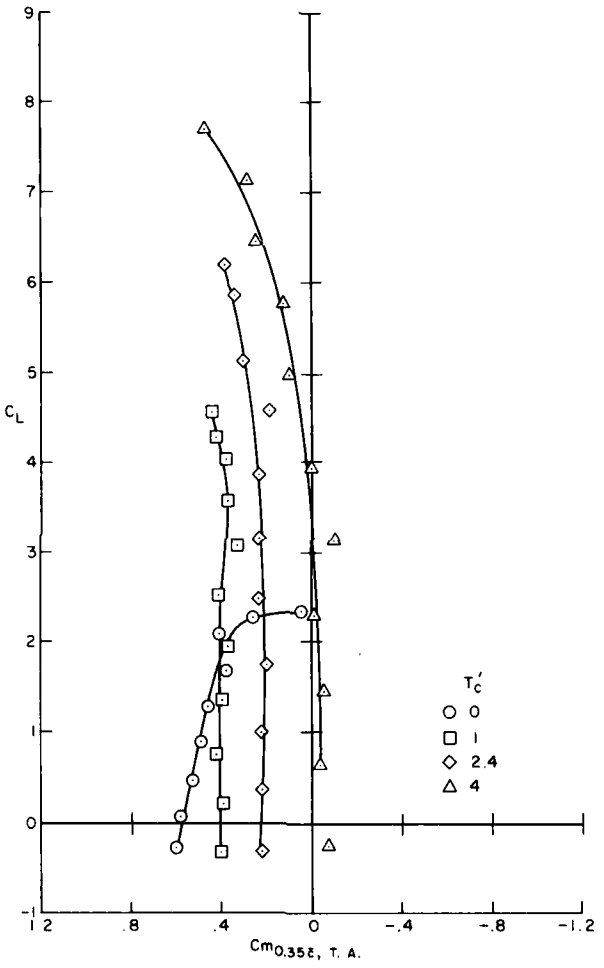

(e) $\delta_{F/V} = 20/9.5$, $i_H = -10$.

Figure 17.– Continued.

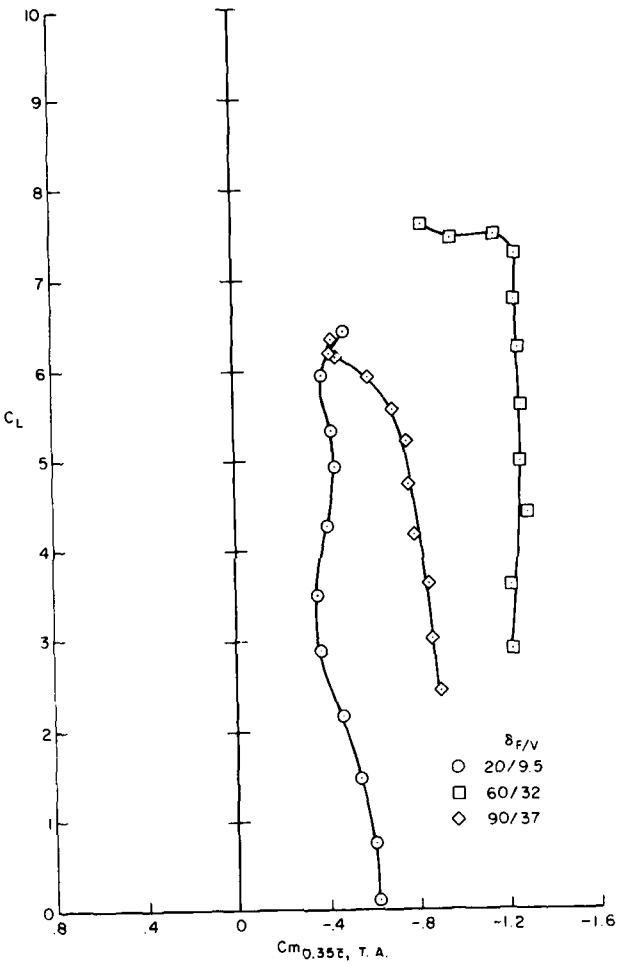

(f) Superposition of tail-off data for a range of flap settings, $T_c' = 2.4$.

Figure 17. - Concluded.

1. Report No. NASA TP-1696 USAAVRADCOM TM-80-A-1	2. Government Accession No. AD-A086 488	3. Recipient's Catalog No.
4. Title and Subtitle **LARGE-SCALE WIND-TUNNEL TESTS OF INVERTING FLAPS ON A STOL UTILITY AIRCRAFT MODEL**		5. Report Date June 1980 6. Performing Organization Code
7. Author(s) Terrell W. Feistel and Joseph P. Morelli		8. Performing Organization Report No. A-7061 10. Work Unit No. 505-10-12
9. Performing Organization Name and Address NASA Ames Research Center and Aeromechanics Laboratory AVRADCOM Research and Technology Laboratories Moffett Field, CA 94035		11. Contract or Grant No. 13. Type of Report and Period Covered Technical Paper 14. Sponsoring Agency Code
12. Sponsoring Agency Name and Address National Aeronautics and Space Administration Washington, DC 20546 and U.S. Army Aviation Research and Development Command St. Louis, MO 63166		

15. Supplementary Notes

Terrell W. Feistel: Ames Research Center
Joseph P. Morelli: Aeromechanics Laboratory, U.S. Army R&T Laboratories (AVRADCOM)

16. Abstract

A unique inverting flap system has been investigated on a large-scale deflected slipstream model in the Ames 40- by 80-Foot Wind Tunnel. The subject tests utilized 33% chord double-slotted flaps on a low-aspect ratio wing that was fully immersed in the propeller slipstream. Evaluation of the flap effectiveness is aided by comparisons with the results of tests of other flap systems on the same twin propeller, twin tail boom STOL utility aircraft mode.

No extreme or abrupt force or moment increments were encountered when the flaps were deflected through a wide range, corresponding to the complete retraction/extension spectrum. The lift and descent capability of the inverting flaps compared very favorably with that of the other flap systems that have been tested on this model, including some with much greater mechanical complexity. As expected, the flaps caused large nose-down pitching-moment increments at the high lift settings; however, the trimmed characteristics are still competitive with those obtained from the more complicated flap systems.

It is believed that these flaps may have promising potential application to the design of relatively simple STOL utility aircraft with improved performance capabilities. In addition, they may merit consideration as retrofits to existing aircraft with less effective flap systems.

17. Key Words (Suggested by Author(s))	18. Distribution Statement
High lift flaps STOL aircraft Aerodynamics Large-scale testing	Unclassified - Unlimited STAR Category - 05

19. Security Classif. (of this report)	20. Security Classif. (of this page)	21. No. of Pages	22. Price*
Unclassified	Unclassified	56	$5.25

*For sale by the National Technical Information Service, Springfield, Virginia 22161

NASA-Langley, 1980